TAMPEREEN TEKNILLINEN YLIOPISTO
TAMPERE UNIVERSITY OF TECHNOLOGY

ANSSI MÄENPÄÄ

DESIGN OF SIX DEGREES OF FREEDOM HYDRAULIC MANIPULATOR FOR UNDERWATER APPLICATION

Master of Science Thesis

Examiner: Prof. Jouni Mattila
Examiner and topic approved by the faculty council of Engineering Sciences on
September 7th 2016.

ABSTRACT

ANSSI MÄENPÄÄ: Design of six degrees of freedom hydraulic manipulator for underwater application
TAMPERE UNIVERSITY OF TECHNOLOGY
Master of Science Thesis, 77 pages, 9 appendix pages
October 2016
Master of Science degree in Automation Engineering
Major: Machine automation
Examiner: Prof. Jouni Mattila

Keywords: Hydraulic manipulator, subsea research, rotary actuator

Research in Arctic regions has increased significantly in the last years. Depletion of natural resources has required the oil and gas companies to search for alternative locations to harvest the natural resources. Arctic subsea environment contains significant territories still untouched. Strong tidal currents and uneven terrain of seabed poses difficult environment for the utilization of resources.

The Academy of Finland has financed multiple research project focusing on the research of the Arctic environment. Project Seaspider focuses on the designing sustainable control systems to enable operation of parallel working manipulators, installed on seabed crawlers operating at the bottom of the sea. These crawlers are designed to surpass ROVs, remotely operated vehicles, operating underwater today. ROV is susceptible to tidal currents and requires to be connected to a surface vessel at all times. The surface vessel provides power and control to the underwater vehicle.

The purpose of the thesis project is to design a hydraulic manipulator capable in operation in subsea environment. Thesis project is based on a Master's thesis by Mikko Siven [1] titled "Design of hydraulic underwater robotic arm". The designed manipulator is used in the implementation and testing of the control system. Commercial components, such as HIAB loader crane as well as commercial actuators, such as rotary actuators, are used in the design. The design project focuses on the design and validation of mechanical parts as well as modification of the commercial components to accomplish six degree of freedom manipulator for subsea environment.

TIIVISTELMÄ

ANSSI MÄENPÄÄ: Kuuden vapausasteen hydraulisen manipulaattorin suunnittelu vedenalaiseen käyttöön
TAMPEREEN TEKNILLINEN YLIOPISTO
Diplomityö, 77 sivua, 9 liitesivua
Lokakuu 2016
Automaatiotekniikan DI tutkinto-ohjelma
Pääaine: Hydrauliikka ja automatiikka, koneautomaatio
Tarkastaja: Prof. Jouni Mattila

Avainsanat: hydraulinen manipulaattori, vedenalainen tutkimus, vääntömoottori

Arktisen alueen tutkimus on kasvanut viime vuosina huomattavasti. Syynä tähän on etenkin luonnonvarojen ehtyminen sekä uusien esiintymien vaikea löytäminen. Arktisen alueen merenpohjassa on huomattavan suuria, täysin tutkimattomia alueita. Öljy- ja energiayhtiöt ovat pitkään yrittäneet päästä käsiksi merenpohjan öljyesiintymiin sekä mineraaleihin. Luonnonvarojen hyödyntämistä vaikeuttavat vaativat olosuhteet; suuret merivirrat sekä kova ja epätasainen merenpohja.

Suomen Akatemia rahoittaa useita tutkimusprojekteja keskittyen arktiseen tutkimukseen sekä operointiin vedenalaisissa olosuhteissa. Seaspider-projekti keskittyy kestävien ohjausjärjestelmien suunnitteluun vedenalaisille rinnakkaistoimiville manipulaattorille, jotka on asennettu merenpohjassa liikkuviin traktoreihin. Traktorien tarkoituksena on osittain korvata nykypäivänä käytössä olevat ROV vedenalaiset sukellusalukset etenkin merenpohjan tutkimuksessa. ROV altistuu merivirroille ja on riippuvainen merenpinnalla sijaitsevasta aluksesta, joka syöttää jatkuvasti virtaa ROV:lle. Myös vedenalaisen aluksen ohjaus tapahtuu pinta-aluksesta käsin.

Diplomityön tarkoituksena on suunnitella vedenalaisiin olosuhteisiin soveltuva manipulaattori, jota voidaan hyödyntää ohjausjärjestelmän suunnittelussa sekä testauksessa. Diplomityö on jatkoa Mikko Sivenin aikaisemmin julkaistulle diplomityölle "Vedenalaisen hydraulisen puomin rannemekanismin suunnittelu". Manipulaattorissa hyödynnetään kaupallisia osia, kuten hydraulista HIAB kuormanosturia sekä kaupallisia toimilaitteita, kuten hydraulisia vääntömoottoreita. Suunnitteluprojekti perustuu kaupallisten komponenttien yhdistämiseen toimivaksi kuuden vapausasteen kokonaisuudeksi, joka soveltuu käytettäväksi vedenalaisissa olosuhteissa.

PREFACE

This Master of Science thesis was constructed under the department of Intelligent Hydraulics and Automation (IHA) at Tampere University of Technology. The study is part of a research project Seaspider.

I would like to thank my supervisor, Professor Jouni Mattila, for providing the subject of the thesis. The project combined my major of machine automation and my minor of machine design and was an excellent subject as thesis project. The help and support from colleagues and fellow thesis workers at IHA was very important and much appreciated. Finally, I would like to thank my friends and family for their support during the project.

Tampere, 10.10.2016

Anssi Mäenpää

TABLE OF CONTENTS

TERMS AND DEFINITIONS

COTS	Commercial Off-The-Shelf
DoF	Degree of Freedom
FEM	Finite Element Method
FoS	Factor of Safety
HPU	Hydraulic Power Unit
IHA	Tampere University of Technology department of Intelligent Hydraulics and Automation
IP	International Protection
NBR	Nitrile rubber
ROV	Remotely Operated Vehicle
TUT	Tampere University of Technology
WHMAN	Water Hydraulic MANipulator

1. INTRODUCTION

Subsea exploration has increased and especially in the Arctic, focus in the utilization of natural resources is increasing. Decreasing price of oil and challenging environmental aspects of the region impose a requirement for new and cost-effective solutions in drilling and extraction of resources.

Large oil and gas companies have been trying to benefit from the substantial amount of natural resources located at the bottom of the ocean. However, strong tidal currents and hard seabed require great amount of power and rigid structures from the operating vehicles and machines to enable stable, safe and efficient functioning.

In manipulation tasks where large payloads are present, hydraulics are preferred. Hydraulic actuator has significant power-to-weight ratio compared to, for example, electric actuators. Ability to transfer power for long distances using oil or water as a medium enables lightweight solutions for actuators. That is why hydraulic machines are preferred in seabed exploration.

1.1 Project Seaspider

Seaspider research project is a part of the Academy of Finland's Arctic Academy Programme (ARKTIKO). Project is carried out in cooperation between Aalto University's department of Electrical Engineering and Tampere University of Technology's (TUT) department of Intelligent Hydraulics and Automation (IHA). As stated in the Academy of Finland's website [2], the ARKTIKO aims to acquire knowledge of the Arctic region and especially to understand the affection of climate change to the region. ARKTIKO also aims to strengthen the Finnish Arctic research and retain leading position in the sustainable development of the Arctic [3].

The Seaspider project objective is to design control framework for decentralized heavy-duty hydraulic manipulators [3]. The project faces four main challenges according to project description [3]:

1) The cooperative manipulators must simultaneously grasp the object, move it along a desired trajectory on the environment, exert a pre-specified contact force on the environment, and regulate the internal force in the object

2) The imprecisions in the positioning of the robot base on top of a slowly moving crawler vehicle on an uneven seabed

3) Commercial robot force/moment sensors do not exist on the market for robots with over 500 kg and high contact forces

4) The subsea environment places strong practical limitations on real-time information flow among different vehicles

The main objective of the project is to overcome these challenges. The focus of the project is to implement the control system to a reliable and precise machine. That is why the project focuses on seabed crawlers, which are large vehicles operating at the bottom of the ocean. Figure 1 represents a simplified model of such crawler. Seabed crawlers are presented in section 2.1.1.

Figure 1. *Simplified representation of the seabed crawler [3]*

The research project itself is divided into three parts. The first part includes the development of the control system using a subsystem dynamics-based control design and is carried out by IHA. Second part is about developing a learning-interaction dynamics. These dynamics assist the control system developed in the first part to estimate unmodellable aspects of the control system. The dynamics are established using multi-sensor feedback provided by visual, force and torque sensor data. Second part is carried out by the Aalto University. The last part is about merging results from the two previous parts and demonstrating the outcome. This is carried out in cooperation between interested parties (TUT/Aalto).

1.2 Scope and structure of the thesis

The thesis project is continued from previously published Master's thesis by Mikko Siven [1]. Thesis focuses on the mechanical design and structural validation of spherical wrist which was not reviewed in Siven's thesis.

The scope of the thesis project is to design a hydraulically operated six degree of freedom manipulator. The designed manipulator consists of commercial HIAB loader crane as well as custom made three Degree of Freedom (DoF) spherical wrist to create fully functional manipulator to perform underwater. This manipulator is then used as a tool in the design of the subsystem dynamics-based control system presented in the Seaspider project description [3]. Main focus of the thesis is in the mechanical design of the 3 DoF spherical wrist. Structural validation is acquired in order to design a stiff and reliable spherical wrist for the underwater manipulator.

Chapter 2 focuses on the available applications on the market in the field of underwater exploration and manipulation. Chapter 3 lists all of the requirements of the design process including environmental and performance requirements in addition to specific components required. Chapter 4 focuses on the concept design of the underwater manipulator. Description of the commercial components used are provided. Two concept designs of the spherical wrist are reviewed. Chapter 5 is about the actual design of the 3 DoF spherical wrist. The chapter provides detailed presentation of each link of the spherical wrist. Chapter 6 focuses on structural validation of previously designed wrist. Also basic theory of finite element method is provided. Chapter 7 is about providing the list of aspects to consider and possible modifications required for the whole underwater manipulator in order to enable submerging of the manipulator. Chapter 8 is the summary of the thesis including ideas for possible future development.

2. UNDERWATER MANIPULATORS

In subsea exploration and work cycle, various type of tools are used. Typical subsea work could be drilling, trenching, jetting or just picking up an object. To enable flexible movement of the tools for these tasks, joints and arms are required. That is why manipulators are preferred in subsea working vehicles. These manipulators enable variable working distance between the vehicle and the object. Also with multiple DoF enabled by the manipulators, tools can be positioned to difficult locations within the manipulator reach or workspace.

2.1 Underwater working vehicles

In subsea environments, manipulators are attached to carrying vehicles that act as a base for the manipulator. Mobile base enables infinite workspace for the manipulator. Carrying vehicle can be submarine-like ROV connected to support platform via tethers or seabed crawler operating on the ocean floor.

2.1.1 Remotely operated vehicle

Remotely operated vehicle (ROV) is a small underwater vehicle designed to be used in subsea exploration and installation and removal works. Typical tasks for ROV include exploration, drill support and construction tasks depending on the setup and accessories of the ROV [4].

ROVs are used in applications, where presence of an operator is not possible due to various reasons. The most important factor is the safety of the operator underwater. In depths ranging in kilometres, the pressure compensation between the pod and the ambient water is very difficult and resource-consuming. That is why remote-controlled ROVs are preferred. ROV can range from a small pod equipped with camera to work class ROV equipped with manipulators and tools.

Soil Machine Dynamics Ltd (SMD) manufactures a wide range of ROVs to be used in number of applications. Figure 2 represents typical work class ROV, named "Quasar", by SMD. Work class ROVs are focused in this thesis for the reason that those are usually

equipped with one or two manipulators, which is the main focus of the thesis design project.

Figure 2. *"Quasar" work class ROV by SMD*

Quasar is medium-range work class ROV by SMD. The depth rating of the Quasar is 4000*msw* or "meters of sea water". Quasar has two hydraulic Shilling Robotics manipulators installed with a total lift capacity of 250*kg* at full reach.

ROVs are operated from a ship or vessel using electric umbilical cables or "tethers". These cables transfer power and control data to the ROV. The operator controls the manoeuvring and manipulation of the ROV by controlling the thrusters and manipulators attached. Sensor and video data can be transferred back to the vessel for feedback and analyzation purposes.

Problem with the usage of ROVs in harsh environments is the "tether" connected to the supporting vessel or platform. As stated in [5], the cable is subject to motion of the vessel. This phenomena can be addressed especially in lower depths where the current is strong. In addition, strong currents create a challenge for the ROV by introducing undesired movement. ROVs are prone to the water masses moving the vehicle and require extra power from the vehicle itself to stay on the desired location.

Seabed crawler is one type of ROV, operating at the bottom of the ocean. Seabed crawlers are used in trenching, seabed exploration and mineral collecting. Because of solid working ground, seabed crawlers are not as prone to environmental effects than typical submarine-like ROVs. Figure 3 represents a type of seabed crawler, SMD CBT1100, designed for subsea trenching.

Figure 3. *SMD CBT1100 trencher [6]*

As can be observed in figure 3, the crawler is equipped with a manipulator. Manipulator has a maximum reach of 7.0m with lift capacity of 430kg at full reach. The structure of the manipulator in CBT1100 is similar to the Seaspider underwater manipulator. Underwater manipulator structure is reviewed in chapter 4.

Seabed crawlers are also connected to the surface vessel using tethers, but unlike submarine ROV, seabed crawler can be equipped with power source to provide power to the actuators of the vehicle. Control data and feedback signals are provided between the crawler and surface vessel.

Large seabed crawlers are fairly new technology due to demanding environmental constraints. Uneven seabed results in a positioning errors with the crawler which has to be taken into account in the control of the vehicle. Also compared to submarine ROV, seabed crawlers must endure longer periods of time submerged. Submerging and raising the crawler is much more demanding than with the submarine ROV.

2.2 Electric manipulators for ROVs

There are few fully electric manipulators on the market. For a number of reasons, hydraulic manipulators are still superior choice in the ROV business.

Electric manipulators rely either on servo motors in the joints of the arm to create revolute joints or on electric linear actuators, such as cylinders, to enable robotic movement of the manipulator. One example of an electric manipulator used in the ROV industry is ARM 7E electric manipulator by ECA group [7], presented in figure 4. ARM 7E has maximum reach of 1790mm with lift capacity of 40kg at full reach.

Figure 4. *Eca group ARM 7E electrical manipulator*

Electric manipulators have inferior power-to-weight ratio compared to hydraulic counterparts [8]. Large electric servomotors and actuators require much more space than hydraulic actuators, thus increasing the weight of the manipulator. Electric manipulators on the market have a maximum payload capacity of approximately 40kg at reach of 1.7 metres, when hydraulic counterpart with same weight and maximum reach can handle up to 159kg payload [9]. Payload capacities are determined on dry ground.

To classify the electric component's ability to withstand submerging, IP codes are generated. International Protection (IP) codes are standardized method for electrical devices to represent the capability of the device to withstand environmental constraints. IP codes are defined in the standard SFS-EN 60529 [10]. IP codes are presented in two numbers and with possible extra lettering, for example "IP23CS", to provide information about the housing properties of the device. Descriptions of IP code digits are presented in tables 1 and 2. First digit after letters IP represents the device's capability to withstand dust and small particles. The second digit of the IP code represents the housing's capability to protect the device against water.

Table 1. *Designation of first digit of IP code according to [10]*

Digit	Description
0	Non-protected
1	Protected against solid foreign objects of 50*mm* ⌀ and greater
2	Protected against solid foreign objects of 12,5*mm* ⌀ and greater
3	Protected against solid foreign objects of 2,5*mm* ⌀ and greater
4	Protected against solid foreign objects of 1,0*mm* ⌀ and greater
5	Dust-protected
6	Dust-tight

Table 2. *Designation of second digit of the IP code according to [10]*

Digit	Description
0	Non-protected
1	Protected against vertically falling water drops
2	Protected against vertically falling water drops when enclosure tilted up to 15°
3	Protected against spraying water
4	Protected against splashing water
5	Protected against water jets
6	Protected against powerful water jets
7	Protected against the effects of temporary immersion in water
8	Protected against the effects of continuous immersion in water

Because the ROV manipulators are required to withstand submerging for practically infinite amount of time, IP68 class housing protection is required. IP68 protection class is also required and pursued in the thesis manipulator design.

2.3 Hydraulic manipulators

Hydraulics are widely used in applications where high payloads are required. With high power-to-weight ratio, hydraulics are superior choice compared to, for example, electricity especially in applications, where high payloads are required.

With hydraulic manipulators, all the components required for the operation, such as hydraulic power unit, valves and oil reservoir, can be submerged with the manipulator. This is very common practice in deep-sea environments and with ROV systems where compact design is preferred. Components still require external power and control, but the power demand is not nearly as much as with electric manipulators. With depths lower than 50

metres, and with only one or two actuators, it is possible to leave power unit and additional components to the surface and use hoses to transfer hydraulic power underwater to the actuators [1].

Shilling robotics hydraulic manipulators are used in multiple ROVs in subsea exploration and work duties. Schilling manipulators range from 682*mm* to 1922*mm* according to maximum reach and 68*kg* to 250*kg* according to lift at full reach on dry ground. Figure 5 represents a medium lift manipulator of Schilling manipulator product range with lift capacity of 159*kg* at full reach of 1806*mm*. Manipulator can be submerged 3000 metres underwater [9].

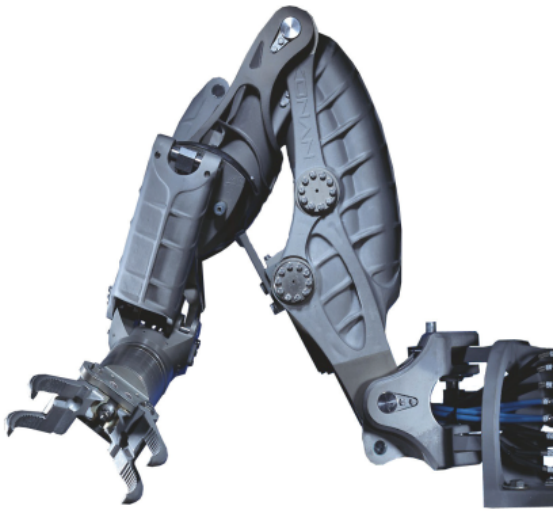

Figure 5. *Shilling Robotics Conan 7P hydraulic manipulator*

All of the Schilling manipulators are hydraulically powered with two types of control systems; position or rate control [8]. With position control, the operator determines the position of the end-effector using a master arm that is a small replica of the manipulator with corresponding analogues in the actual manipulator. With rate control, the operator determines the velocity of the manipulator using a joystick. The control system calculates the required actions on manipulator actuators according to the rate control.

Advanced version of the master-slave manipulator system is the force-feedback controlled system. In force feedback controlled system, the manipulator is equipped with force sensors that scale and transfer the measured force data back to the master arm. This way the operator experiences similar feedback from obstacles and objects as the manipulator itself.

Material used in the Schilling manipulators is either titanium or anodized aluminium with stainless steel. All of these materials are more or less corrosion resistant depending on the alloy, which makes them obvious choice for underwater applications. Titanium, stainless

steel and anodized aluminium were also considered as the material for the underwater manipulator of the thesis project. Material comparison of the designed underwater manipulator is reviewed in detail in section 5.2.

Most common ROV is a hybrid version of the electrical and hydraulic power. In hybrid ROV, the movement is carried out with electric propellers or thrusters and the manipulator is hydraulically powered.

3. DESIGN REQUIREMENTS

Every design process begins with a definition of requirements. Requirements are the guidelines which the completed design has to follow or parameters which the completed design has to achieve. Requirements can be divided into functional and non-functional requirements [11]. Functional requirements describe the behaviour of the system and are something that can be measured from the system. Functional requirements include possible inputs and outputs as well as behaviour of the system. Non-functional requirements are related to safety, cost and certain technologies used in the system.

Functional requirements of the underwater manipulator are part of the control system design of the manipulator. Thesis project focuses on the physical and mechanical properties of the system as well as technology used in the system. Both, functional and non-functional requirements, are created, but focus being in the non-functional requirements. Environmental constraints affect the performance of the system as well as the design of the system and that is why it is covered in requirements section of the design project. With accurate description of requirements, the actual design process is faster and more straightforward because of definitive guidelines to follow. Accurate requirements are also not open to interpretations. Well defined and accurate requirements provide traceability and reliability for the designed system.

Design process of this thesis focuses on the design of the mechanical parts of the spherical wrist. Joint actuators were chosen and acquired prior to the project. Possible alternatives for the joint actuator are compared briefly in this section.

3.1 Structural requirements

The underwater manipulator is required to be constructed from two parts: arm and wrist. This is common division in manipulator and robotic applications. The arm is combination of long links and spherical wrist connected to it is shorter with usually three DoF enabled by three joints. In the thesis project, the arm is considered to be commercial loader crane and the wrist is designed to be attached to it. Figure 6 represents the alignment of joints in spherical wrists in general.

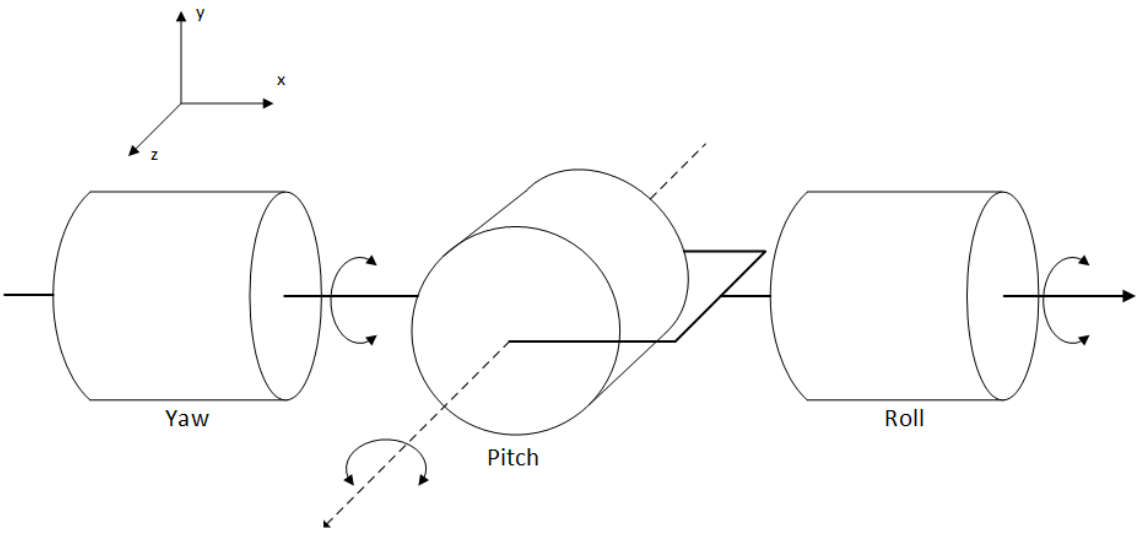

Figure 6. *Spherical wrist joint alignment*

Joints 1 and 3 are aligned in same orientation to each other. Joint 2 is perpendicular. In robotic applications, joints are labelled "Yaw", "Pitch" and "Roll" from joint 1 to 3.

3.2 Environmental constraints

Because the Seaspider project is about designing a sustainable machine for subsea tasks, especially in the Arctic, the environmental requirements are supposed to follow these aspects and provide a reliable solution to be used in that environment. Subsea environment acquires few important requirements for the design to consider.

The manipulator is submerged in the ocean. For that reason, the design has to be water-proof as well as leak-proof. The depth rating of the commercial ROV applications vary from $50m$ cable burial applications all the way to $4000m$ deep sea ROV [4]. Underwater manipulator designed in this thesis is decided to be able to be submerged in $100m$ depth. Same depth rating was used in the Siven's Master's thesis [1], which was baseline for the current design project. Because the manipulator is developed for research purposes without any commercial interest, the $100m$ is determined to be enough to display the challenges that submerging of the manipulator has to withstand.

In 100 meters underwater, hydrostatic pressure has to be taken into consideration. Hydrostatic pressure is a stress that is caused by the water mass and it affects the maximum stress, the system has to endure. Hydrostatic pressure p_h can be calculated using equation 1:

$$p_h = \rho g h \tag{1}$$

Where:

- ρ Density of the fluid
- g gravitational acceleration
- h depth from the sea level

With $100m$ depth, the hydrostatic pressure is approximately $981\ 000Pa$ which is about $10bar$. This amount of pressure doesn't have affect on the metallic chassis parts of the manipulator but might have effect on the sealing solutions and other non-metallic parts in the structure. With sealing solutions, the evaluation is critical so that structure will remain waterproof even in maximum depth.

Seawater having high concentration of salt imposes few challenges. Salt in the water corrodes the materials used in the manipulator and corrosion resistance is taken into account. Corrosion resistant metals are chosen in comparison for the mechanical parts of the manipulator.

Seawater has a specific temperature range depending on the location. This temperature range is taken into account in the sealing solutions and in transferring the hydraulic fluid. Ambient temperature affects the viscosity of the fluid and therefore the performance of the system. Temperature in the Arctic ocean is measured to be anywhere between -2 and +10 degrees Celsius [12]. Without proper insulation, the temperature affects the performance of the system.

3.3 Joint actuators for the spherical wrist

With 3 DoF of motion defined in the requirements, the designed spherical wrist requires three actuators. Every actuator enables one DoF. Actuators form joints and between joints, there are links.

In robotic applications in general, the actuators have limited work envelope. That is why in the spherical wrist design, the actuators are chosen as hydraulic rotary actuators. Rotary actuator provides compact design with fixed maximum rotation to achieve robotic work envelope for the manipulator. Hydraulic actuators are chosen because of high power-to-weight ratio and power requirement determined in [1].

Because of limited resources for the design project, commercial actuators were chosen. The decision was considered between two types of rotary actuators; vane actuator and linear rotary actuator. Both of these are demonstrated briefly in this chapter. Section 5.1.1

describes the chosen actuator for the manipulator in detail.

First choice for the actuator was a vane actuator. Vane actuator was already used in another manipulator design project WHMAN ("Water Hydraulic MANipulator") [13] in TUT in the department of IHA. Vane actuators were also considered in Siven's wrist design [1].

Vane actuator consists of two hydraulic chambers and rotating vane connected to output axis. Hydraulic pressure difference in the chamber rotates the vane and thus the output axis providing rotary movement of the actuator. Simple design and mechanism provides reliable solution especially in mobile and robotic applications. Figure 7 represents vane actuator type SS by Micromatic [14].

Figure 7. *Micromatic SS rotary actuator [14]*

SS vane actuators considered for the spherical wrist in [1] were SS-8 actuator. SS-8 has a total width of 297mm, weight 35kg and has a maximum torque output of 2440Nm.

Because the vane actuator structure does not have mechanical parts, such as gears, the actuator does not have any backlash. However, the problem with vane actuators, especially in manipulator applications, is that the actuator tends to leak from one chamber to another. Leakage affects the manipulator's ability to hold the payload still. The payload starts dropping undesirably because hydraulic medium is moving from one chamber to another causing the output axis to rotate. The problem can be minimized by using load-holding valves. Figure 8 represents the principle of vane actuator chambers with one vane [1].

Another problem with the vane actuator is the maximum rotation angle. Without additional gear mechanisms, complete circle of 360 degrees cannot be accomplished. In spherical wrist design, full circle rotation of the joint is pursued.

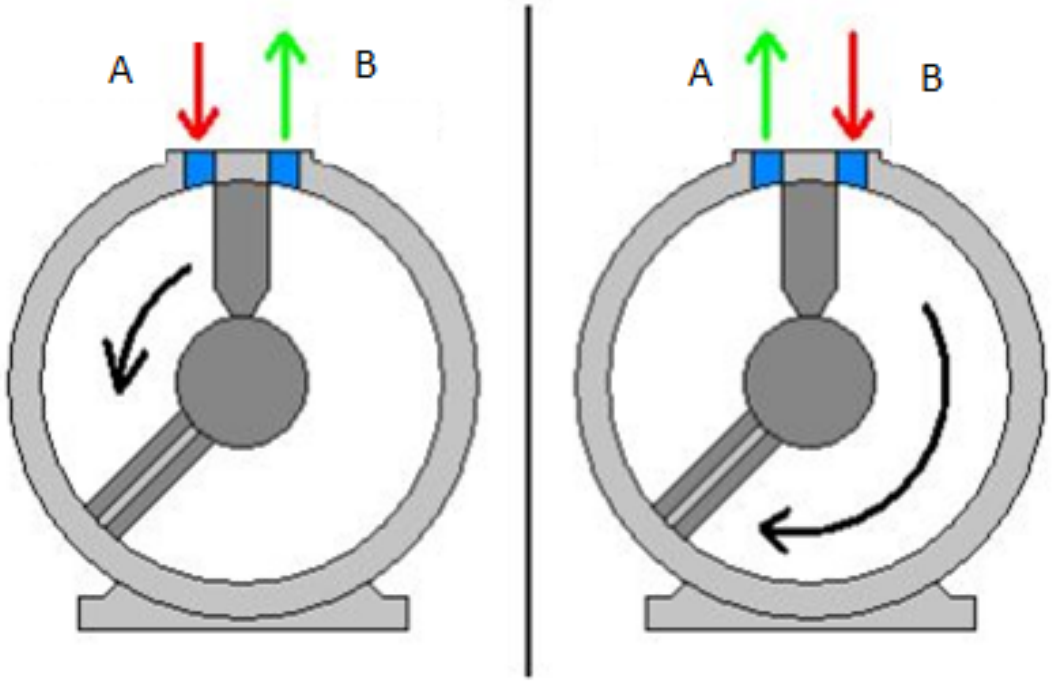

Figure 8. *Schematic of the vane actuator*

Another type of rotary actuator reviewed was linear rotary actuator. Linear rotary actuator combines the linear force of a hydraulic cylinder and the rotary action of a hydraulic motor. Figure 9 represents a cross-sectional view of an Eckart E1 rotary actuator. Eckart rotary actuators were considered for the manipulator.

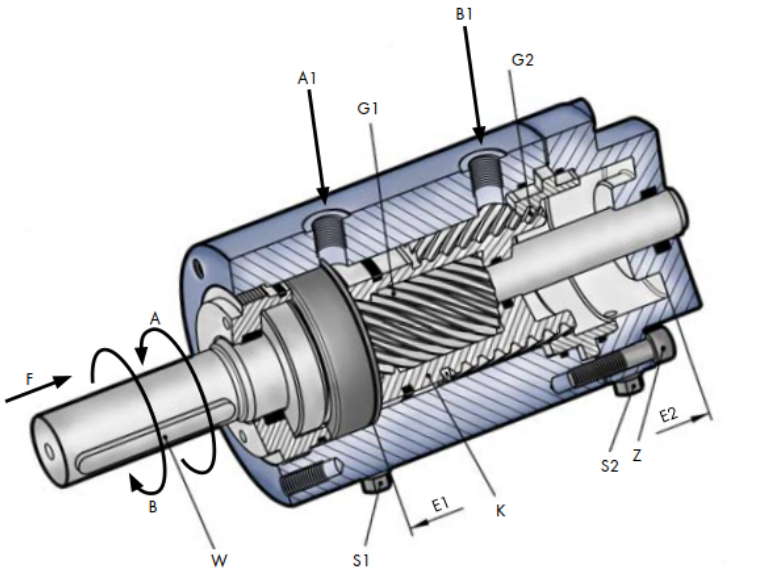

Figure 9. *Eckart E1 rotary actuator [15]*

As can be seen from the picture, rotary actuator consists of helical gears to convert the linear movement of the hydraulic cylinder to rotary movement of the output interface. When hydraulic power is applied to cylinder chamber port A1, the cylinder rotates due to

gears machined on outer surface of the cylinder (labelled G2 in figure 9). Second pair of gears are machined on the cylinder piston (G1 in figure 9). These gears are perpendicular to first set so they rotate in anti-parallel direction to the cylinder which is also the direction for the output interface.

Hydraulic rotary actuator costs about one third compared to vane actuator with similar torque output. Eckart E3 rotary actuators were chosen for the spherical wrist. Eckart E3 actuator has a torque output 2500Nm and a weight of 57.7kg.

With mechanical gears inside, the actuator is able to hold the load even without continuous hydraulic power. Mechanical gears also introduce backlash to the system. Backlash can be minimized with proper control system compensation. Eckart E3 actuator has a backlash of 20 angular minutes or 1/3 degrees at the end position.

3.4 Payload

In design projects in general, required payload is determined before the actual design phase. Required payload is based on the application, tools and typical work cycle of the designed manipulator. In practice, payload requirement is the maximum weight that the manipulator has to be able to lift in its workspace.

In this underwater manipulator design project, the approach was that the maximum payload is determined after the concept design phase. Required payload affects the actuators used in the manipulator. In this case, the actuators were already chosen prior to the design.

The spherical wrist is designed to be attached to commercial loader crane to replicate the manipulator used in the seabed crawlers. Figure 10 is a zoomed image of the seabed crawler manipulator.

Figure 10. *Manipulator of the seabed crawler CBT1100*

Payload capacity of the underwater manipulator is determined based on the lift capacity of the commercial loader crane. In IHA heavy lab, a HIAB XS 033 CLX loader crane is used as the arm of the manipulator. Loader crane is equipped with two telescopic booms with a maximum reach of 6.1 metres and a payload capacity of 410kg in its workspace. The payload capacity of the spherical wrist is maximized based on this payload capacity.

3.5 Underwater manipulator requirements

Requirements of the underwater manipulator system mechanical design are gathered in one table. Requirements are reviewed in previous sections. Table 3 provides classification of requirements into functional and non-functional requirements.

Table 3. *Underwater manipulator requirements*

Requirement	**Type**	**Description**
Req01	functional	Minimum depth capacity of the underwater manipulator shall be 100m underwater
Req02	non-functional	The arm of the underwater manipulator shall be commercial loader crane
Req03	non-functional	The wrist of the underwater manipulator shall be 3 DoF spherical wrist
Req04	non-functional	The actuators of the spherical wrist shall be Eckart E3 hydraulic rotary actuators
Req05	non-functional	The underwater manipulator shall be corrosion resistant
Req06	non-functional	The payload capacity of the spherical wrist shall be maximized based on the torque output of the Eckart E3 hydraulic actuators
Req07	non-functional	Factor of Safety of 1.5 shall be used in structural validation
Req08	non-functional	The underwater manipulator shall be IP68 class protected

Table is later reviewed again in the final phase of the design to validate the underwater manipulator design based on these requirements. The review of the requirements is presented in chapter 8.

4. DESIGN OF THE UNDERWATER MANIPULATOR

The underwater manipulator designed in this thesis is divided into two parts; the arm and the wrist. This division of the manipulator makes it easier to define joints and links between the joints. The arm is HIAB XS 033 CLX loader crane and the wrist is designed to be installed to the crane.

4.1 Manipulator structure and its DH parameters

The underwater manipulator working envelope, as in manipulator applications in general, is optimized to accomplish largest possible area, the manipulator can cover. This enables the execution of tasks in multiple environments. In industrial robotic applications, full spherical working envelope is pursued.

Degrees of freedom in manipulator and robotic applications are described as the end-effectors capability to move in global 6 DoF space. The joints in the manipulator enable the movement in space. In joint actuator space, the number of joints describe the number of DoF for the manipulator. The underwater manipulator designed in the thesis project has 8 DoF in actuator space. In Cartesian space, the manipulator is designed so that 6 DoF working envelope is achieved.

There are total of seven actuators and joints in the underwater manipulator. However, joints two and three can only rotate according to identical axis, so they provide only one DoF for the manipulator. That is why the underwater manipulator is described as six DoF manipulator. Six DoF means, that the end-effector can move and rotate on any plane in three dimensional Cartesian space.

In order to achieve easily understandable representation of the manipulator, a reasonable division is required for the structure. Division of structure also enables the structural validation divided to each part of the manipulator. Without clear division, defining loads and forces inside the structure would be difficult and in worst cases, inaccurate.

The underwater manipulator is divided into 7 parts. These parts are called "links". A link can consist of multiple parts but the main property is that the link is considered to be one rigid structure. Between links, there are joints. Joints connect rigid structures to each other. Labelling of the joints and links can be observed in figure 11. First joint is located

on the base of the HIAB loader crane and after joint 1 is link 1 and so on.

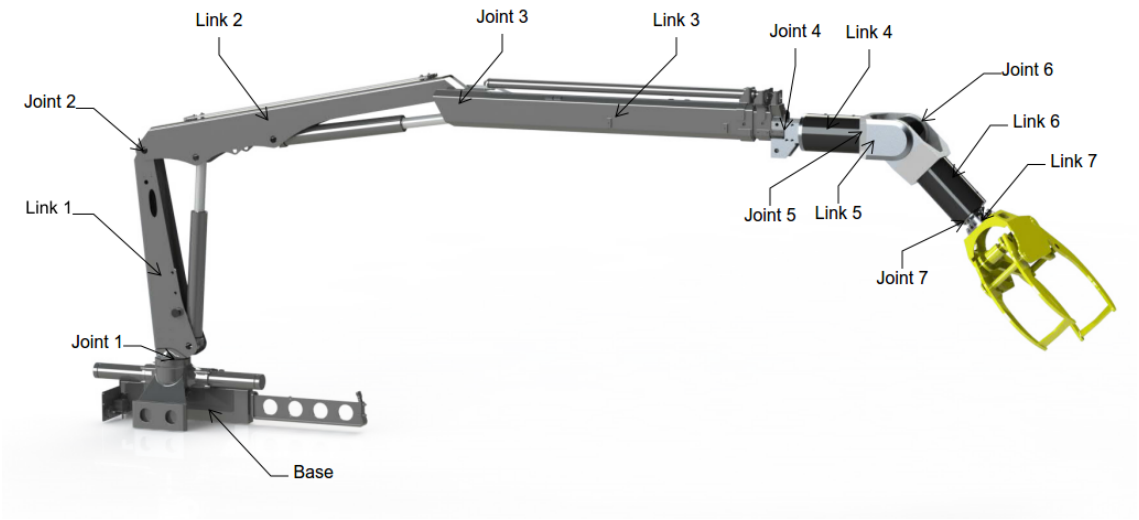

Figure 11. *Manipulator joint structure*

In the underwater manipulator, joints are hydraulically powered. Hydraulic actuators are either hydraulic cylinders, as in joints 1 through 4 or rotary actuators chosen in section 3.3 (joints 5 through 7).

4.2 HIAB 033

As already mentioned, the arm of the underwater manipulator is HIAB XS 033 CLX B-2 loader crane. Loader cranes are hydraulically operated manipulators designed to be used in simple picking tasks. Loader cranes are used in trucks and forwarders, where the main task is to collect objects and transport those objects to desired location.

HIAB XS 033 CLX consists of 3 booms actuated using hydraulic cylinders. These booms are referred as "Pillar", "Lift" and "Tilt" boom correspondingly. In addition, HIAB loader cranes can be equipped with up to 3 telescopic booms, based on the requirements. These telescopic booms define diameter of the work envelope for the crane. The amount of telescopes also defines the maximum payload for the crane. Based on the maximum payload capacity and the actual available space in the test environment, HIAB 033 for this project were chosen to be equipped with one telescopic boom. Figure 12 represents the HIAB XS 033 CLX loader crane but with the maximum amount of telescopic booms rather than the one telescopic boom chosen for the thesis project.

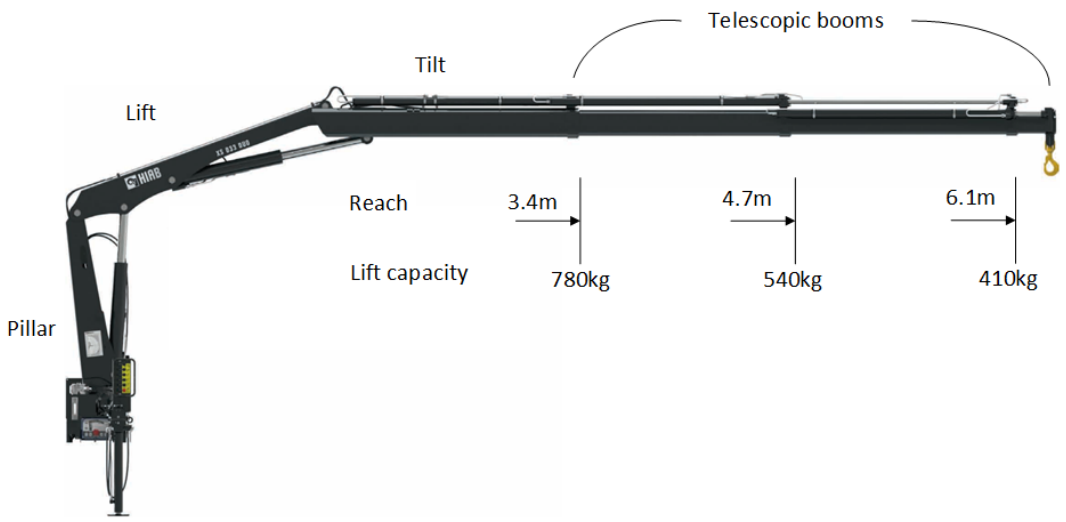

Figure 12. *HIAB XS 033 CLX B-2 loader crane*

With one telescopic boom, HIAB 033 has a working diameter of 4.7 meters and maximum payload of 540kg. These parameters were used in calculation of maximum payload and the worst case load scenarios for the whole underwater manipulator as described in appendices B and C.

In comparison with the workspace and payload capacity, figure 13 represents a scaled workspace of Schilling robotics Conan 7P manipulator with a payload capacity of 159kg at full reach.

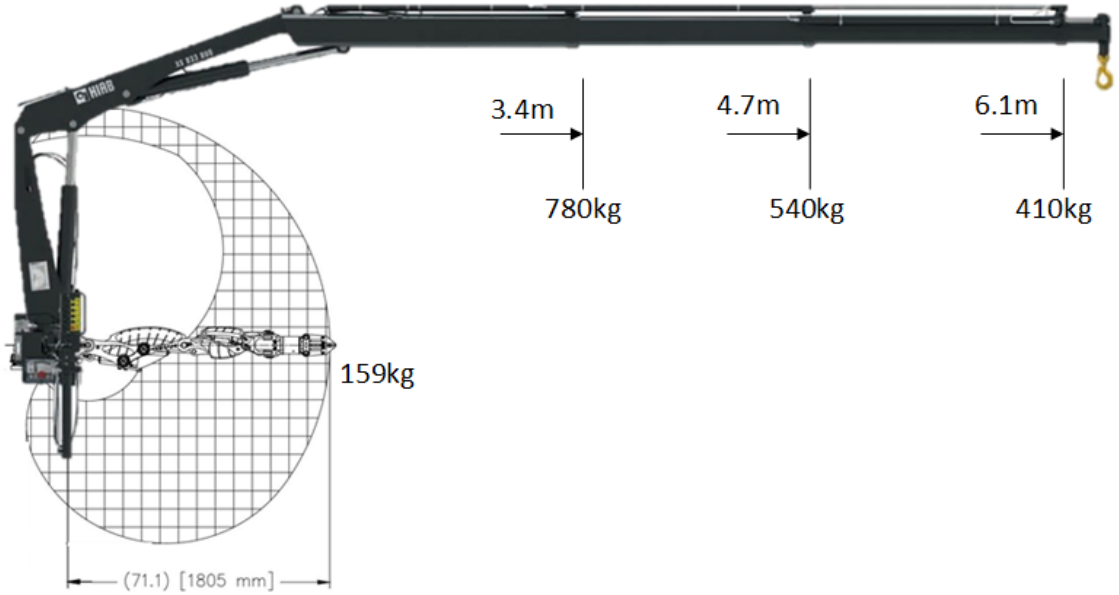

Figure 13. *Workspace comparison of Conan 7P and HIAB 033 loader crane*

4.3 End-effector tooling

Typical underwater manipulator is able to perform pick and place tasks, which is why a hydraulic grapple was chosen as the end-effector tool of the manipulator. Hydraulic grapples are used in forestry, particularly in forwarders. Grapples are used to pick and collect timber from the ground to the forwarder to be transported to a lumber yard. Forestry grapples consists of two or more hydraulically powered claws. These claws grip around the tree to pick it up and move.

Tools were compared according to mass and physical size of the tool. Because no specific tasks were not determined before the design project began, the tool were chosen to be smallest possible in order to achieve maximum payload of the manipulator. Vahva B15 hydraulic grapple were chosen because of its lightweight and simple design. Vahva B15 is the smallest in the range of the Vahva grapples [16]. Maximum grappling area of B15 is 0,15 m^2 and it weighs 89kg without load. Figure 14 represents the Vahva B15 grapple.

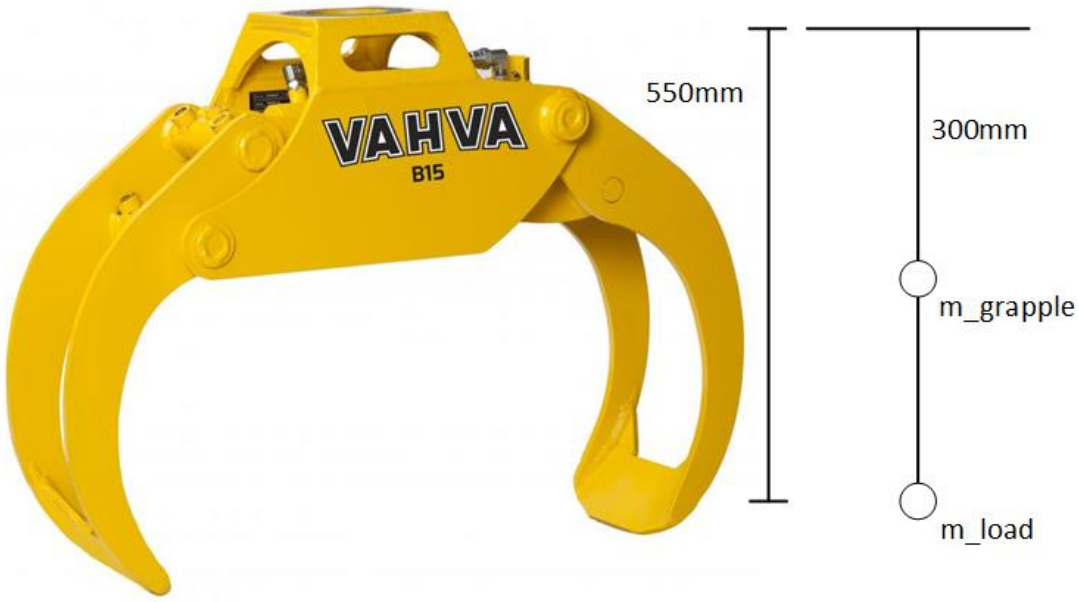

Figure 14. *Vahva B15 grapple [16]*

In calculation of the maximum payload for the manipulator, a CAD model of the grapple was designed to represent the actual grapple as accurately as possible. Dimensions for center of mass and payload distance from the base of the grapple were measured from the model and used in the payload capacity evaluation. These parameters can be seen in figure 14.

4.4 Concept design of the spherical wrist

Before detailed design of the spherical wrist, an initial concept was designed. This concept design was the first functional presentation of the principles and structures of the manipulator. Concept design in general provides solution to some of the requirements by visualizing the operation and typical work cycle of the actual system. As more and more solutions for the requirements are designed into concept, so is the system evolving from concept phase to the actual detailed design.

Spherical wrist concept design was used to analyse the operation of the actuators. Also initial structural validation was performed to evaluate the critical places in the design in terms of stiffness of the design. Material of the structure was also validated during concept design phase, when critical points and maximum stresses were calculated for the structure. Material comparison is reviewed in section 5.2.

Two concepts were considered in the early phase of the design. These concepts were labelled "symmetrical" and "asymmetrical". The difference between the concepts is the middle joint or "pitch" as labelled in robotic manipulators in general.

4.4.1 Asymmetrical concept design

Asymmetrical concept was considered first of the two alternatives. For the lack of rotating connection interface on both sides of the actuator in axial direction, the mechanical parts can only be connected to one side of the actuator. Mechanical parts considered for the asymmetrical design are presented in figure 15.

In asymmetrical design, the joint 6 is constructed from two L-shaped links. These links are the significant links in the structure that differentiate between concept designs so the design is focused on these. L-shaped links are required to be robust and have high elastic modulus to prevent any deformation or inaccuracy in the operation of manipulator. Links are under high load because there is no distribution of load. For that reason, stainless steel alloy 1.4401 (AISI 316) was considered as a material for the design. Steel alloy 1.4401 has an elastic modulus of $210GPa$ and a yield strength of $290MPa$. High yield strength is required to prevent permanent deformation of structure.

links are considered to be constructed using bolted connection in the corner of the link. This simplifies the required parts to basically two plates with required holes machined in them. Additional components such as bearings are not required in this design. However, without significant structural support, bolts used in the connection cannot withstand the payload requirement of the spherical wrist alone.

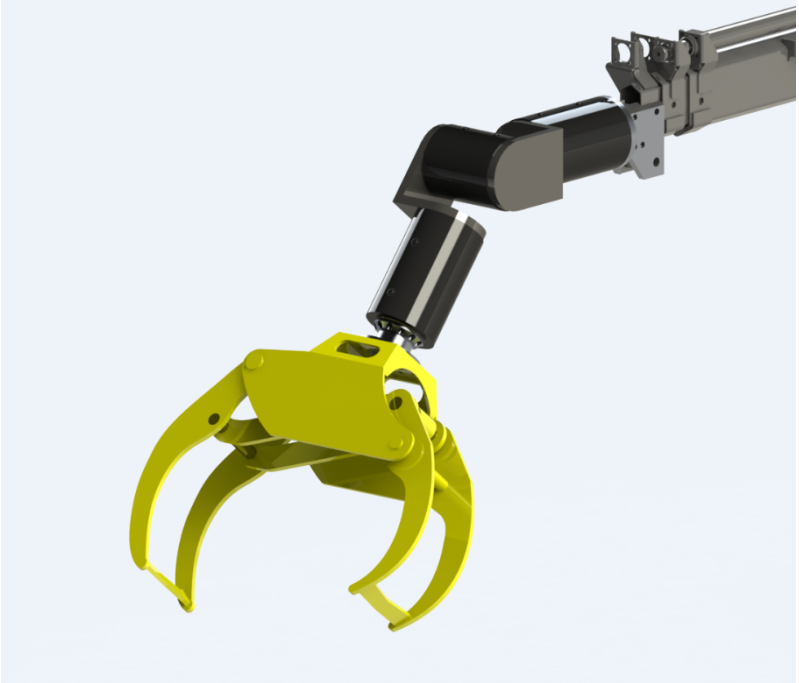

Figure 15. *Underwater manipulator with asymmetrical concept design of the spherical wrist*

4.4.2 Symmetrical concept design

After initial structural validation for the asymmetrical design, loads for the bolted connections were considered abundant for the structure and yielding occurred. That is why division of loads were considered by adding another mechanical links on both sides of joint 6.

Symmetrical design was constructed from asymmetrical design by attaching similar L-shaped links on the other side of the actuator. This created a design that is more common in robotic application and manipulator applications in general. Figure 16 represents the concept design of the manipulator with symmetrical design approach.

Symmetrical design provides stability and stiffness to the structure by dividing the maximum load evenly and for larger area than the asymmetrical design. Aluminium alloy 6082-T6 was considered as a construction material with a yield strength of $240MPa$ because of lower stiffness requirement and lower yield strength requirement compared to asymmetrical design. Aluminium provides lightweight structure and therefore increased payload for the wrist structure.

Symmetrical design requires additional components such as bearings. Eckart E3 rotary actuator does not possess connecting interface on both sides of the actuator, so connecting axis has to be manufactured to link structure itself.

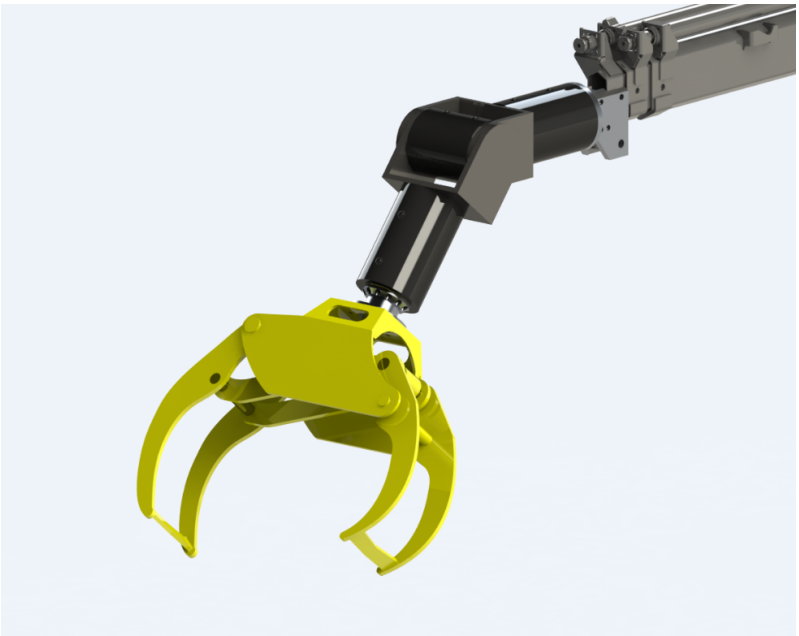

Figure 16. *Underwater manipulator with symmetrical concept design of the spherical wrist*

After concept design phase, symmetrical design was chosen as the approach for the final design. Breakdown of the final design of the manipulator can be observed in section 5.3. Reason for the decision of the symmetrical approach was the stability of structure as well as lower stress in the structure because of increased load distribution.

4.5 Maximum payload of the manipulator

After concept design phase, the payload calculation was carried out. The limiting factors in the payload calculation were the load capacities of the joint actuators. HIAB loader crane were considered to have one limiting payload which were given in data sheet of the crane. With one telescopic boom, HIAB loader crane has the maximum payload capacity of $540kg$.

The model of the underwater manipulator was simplified in payload calculation. Manipulator was considered as a beam with revolute joint on one end. Payload capacity is affected by the weights of the links. Weights were retrieved from the CAD model of chosen concept design of the spherical wrist. These weights were modelled as gravitational forces affecting at corresponding center of masses. Payload capacity of the HIAB is modelled as upward force. Free-body diagram of the simplified model of the manipulator is presented in figure 17.

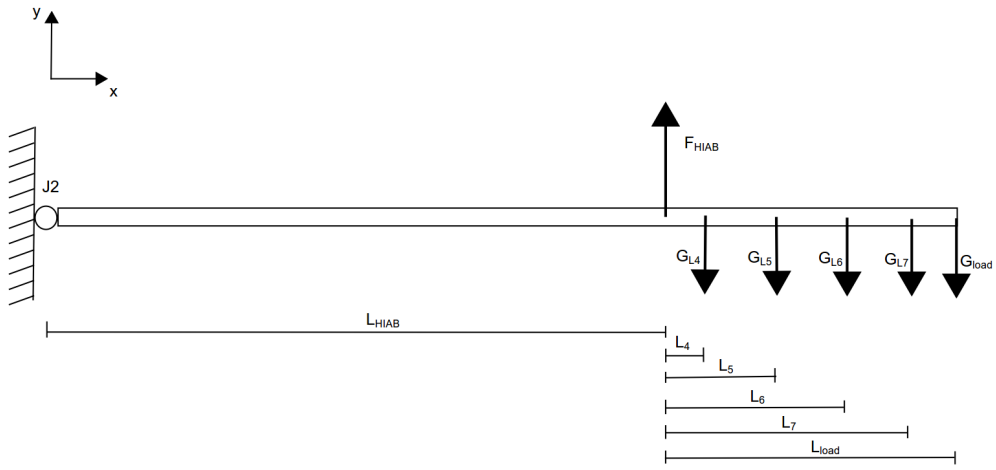

Figure 17. *Free-body diagram of the underwater manipulator links 2 through 7*

Only unknown variable in the equation is the gravitational force of the load G_{load} at the end-effector. Each of the gravitational forces create bending torque to joint 2 labelled in figure. Torque levers were measured from the CAD model. Maximum payload capacity is the sum of these torques reduced as a force in the end-effector, as presented in equation 2

$$G_{load} = \frac{\sum_{i=1}^{n} M_i}{L_{load}} \tag{2}$$

Where:

n	Number of torque elements affecting the joint
M	Torque created by the gravitational force
L_{load}	Distance from joint to the end-effector

Payload capacity of $248kg$ was calculated at the end-effector. The weight of the end-effector tooling has to be subtracted from this capacity to get the actual payload. Corrected payload is of $159kg$ is achieved.

Payload capacity can be given as a single point right at the connecting point of the end-effector. Another way is to display a diagram in which the payload capacity is given as a area in which depends on the distance and direction of the center of mass of the payload. For example, Kuka KR 1000 Titan has a rated payload capacity of $1300kg$ but the capacity is reduced based on the location of the center of mass [17]. Figure 18 represents the Kuka

KR 1000 Titan payload diagram. Kuka KR 1000 Titan has a maximum reach of 3601mm and a weight of 4690kg.

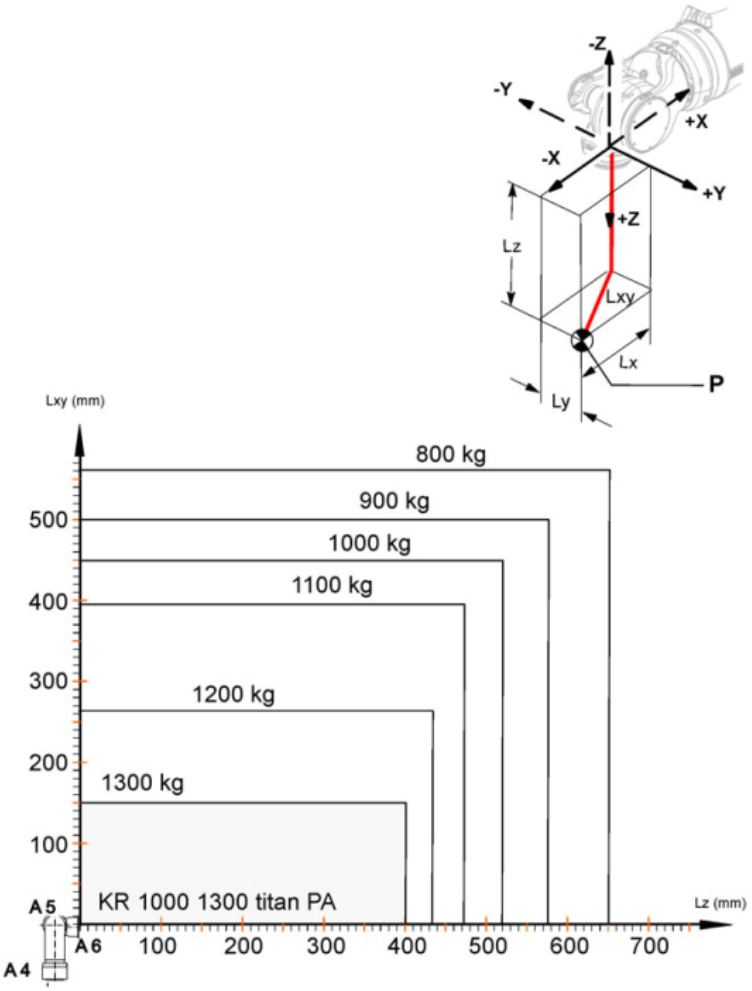

Figure 18. *Payload diagram of Kuka KR 1000 Titan [17]*

In addition to HIAB payload capacity, each of the joint actuators in spherical wrist were examined independently. The rotary actuators have same payload capacity, so the most limiting actuator is the one which has the longest torque arm attached to it. Based on the work envelope of each joint, second joint of the spherical wrist has longest torque arm and therefore limits the payload capacity the most. Free-body diagram of the second joint of the spherical wrist (joint 6 of the underwater manipulator) is presented in figure 19.

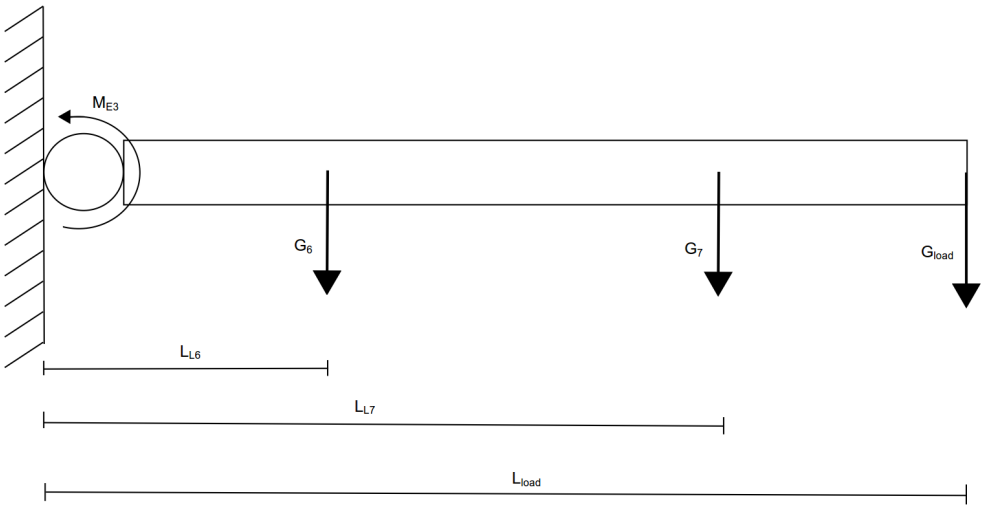

Figure 19. *Free-body diagram of the underwater manipulator links 2 and 7*

Calculation of the payload capacity was carried similarly to previous phase. The chosen Eckart E3 rotary actuator has a maximum torque output of 2500Nm. Maximum payload capacity of 370kg was calculated at the end-effector. After subtracting the weight of the Vahva B15, payload capacity of 281kg was achieved.

To evaluate the payload capacity based on the distance of the load, a graph was created. Figure 20 represents the payload diagram of the underwater manipulator. Blue line represents the payload capacity based on the joint 6 Eckart E3 torque output and red line represents the capacity based on HIAB loader crane payload capacity.

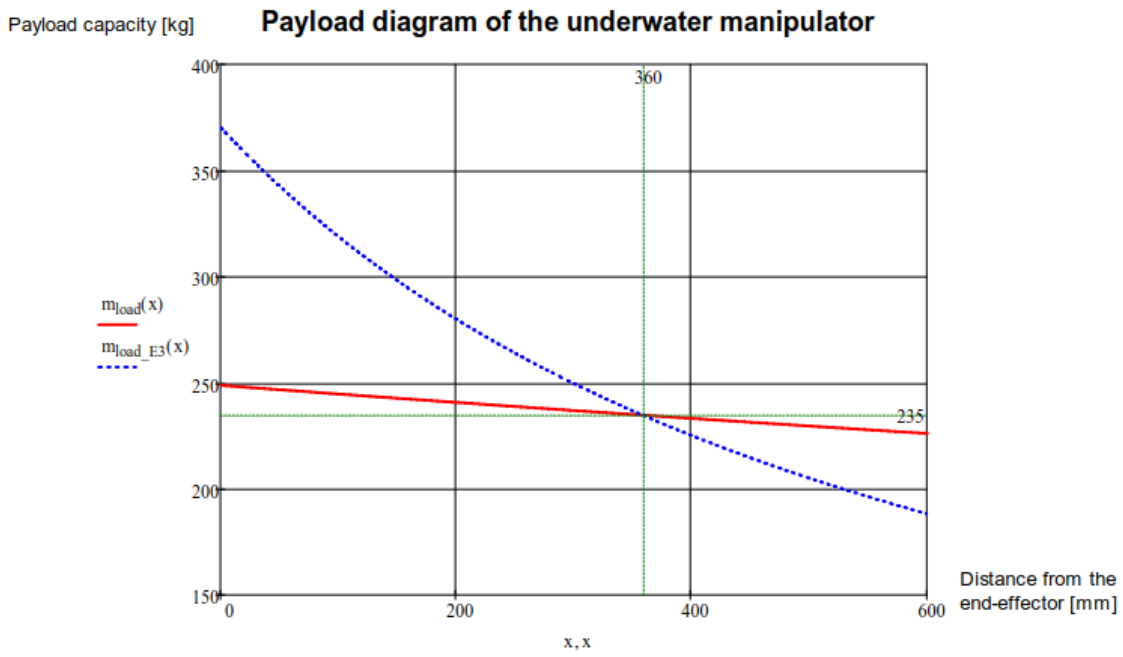

Figure 20. *Payload diagram of the underwater manipulator*

The actual payload of the underwater manipulator is based on the loader crane to the distance of 360mm and after that the capacity is based on the Eckart E3. With the Vahva B15 grapple, the distance of the payload is determined as 550mm from the end-effector. This gives the payload capacity of 196kg and a corrected payload of 107kg.

Calculated payload capacity is determined on dry land. In water, the lift of the water is affecting the payload capacity. Lift depends on the volume of the load object. The calculated payload capacity is then the minimum value, that the spherical wrist can lift.

Because the CAD model is inaccurate in terms of mass properties, the payload capacity is lowered to compensate these inaccuracies. Also the spherical wrist was only a concept design so torque arm parameters are affected throughout the design. Payload capacity is evaluated again and possibly corrected after actual design of the manipulator is carried out.

5. THREE DEGREES OF FREEDOM SPHERICAL WRIST

Main part of the thesis project was to design a 3 DoF spherical wrist using the actuators chosen in the preliminary design phase. Design of the wrist has focused on the mechanical design. Spherical wrist was considered to be attached in the loader crane to create 6 DoF underwater manipulator. This chapter reviews the breakdown of the spherical wrist and describes the design process behind it. Components used in the design are reviewed and material assessment for the final design is carried out. Breakdown and exploded view of the final design of the spherical wrist is included at the end.

5.1 Components

In addition to the actuators chosen for the wrist, number of additional components are required. These components include encoders, sealing elements and bearings. Encoders are used to provide feedback loop for the control system. Sealing elements and bearings are required because of the symmetrical design approach.

5.1.1 Eckart E3 hydraulic rotary actuator

As described in section 3.3, the joint actuators of the spherical wrist are chosen to be equipped with hydraulic rotary actuators. The requirements for the actuators were high torque output, cost-effectiveness, and ability to carry axial weight. Eckart E3 rotary actuators were chosen based on these requirements.

Eckart E3 rotary actuators are hydraulically powered rotary actuators with helical gears. Rotary actuators work with the same principle as hydraulic motor with a main difference of limited rotation. Eckart rotary actuators can rotate only finite amount, where hydraulic motors rotate indefinitely as long as hydraulic power is provided to the motor.

Eckart E3 is stated to be ultra-compact and almost without backlash [18] which is why it was particularly chosen for the wrist. Eckart E3 has lip seals on both ends of its rotating axis to prevent leakage from the structure. This is considered very important in the underwater application. Figure 21 represents the rotary actuator chosen for the underwater

spherical wrist.

Figure 21. *Eckart E3 linear rotary actuator*

Two kind of E3 rotary actuators were chosen. Both of the actuators have same torque output of 2500Nm. Difference between these two is the maximum axial rotation of the actuator. Wrist joints 1 and 3 (manipulator joints 5 and 7) are actuated using E3.150-360°/M with a maximum rotation of 360 degrees. The joint 2 of the wrist (manipulator joint 6) is actuated using E3.150-180°/M, with a maximum rotation of 180 degrees. These parameters are considered to be sufficient for the designed manipulator. Table 4 represents the performance and mechanical properties of the chosen actuators.

Table 4. *Eckart E3 rotary actuator properties*

Parameter	**E3.150-360°/M**	**E3.150-180°/M**
Length	315.4 *mm*	224 *mm*
Diameter	197 *mm*	197 *mm*
Weight	57.675 *kg*	42.739 *kg*
Maximum rotation angle	360 °	180 °
Torque output	2500 *Nm*	2500 *Nm*
Axial load	46000 *N*	46000 *N*
Radial load	44000 *N*	44000 *N*
Operating pressure	210 *bar*	210 *bar*

Actuators were installed in a series in order 360-180-360 based on the maximum rotation angle. Another order of 360-360-180 were also considered. The alternative order would have given work envelope closer to spherical shape, which is usually the purpose in robotic applications. However, the 360-360-180 order would have also reduced the length of the wrist and increased the width of the design significantly which would have made

the structure inadequate for robust and flexible robotic wrist. Choosing the full circle rotation for the second joint would have also made the design prone to collisions between the mechanical parts and that way caused undesired stress to the structure. Objective was to create as close to a spherical work envelope as possible. With chosen actuators, hemispherical work envelope was achieved. Figure 22 represents the working envelope designed for the spherical wrist.

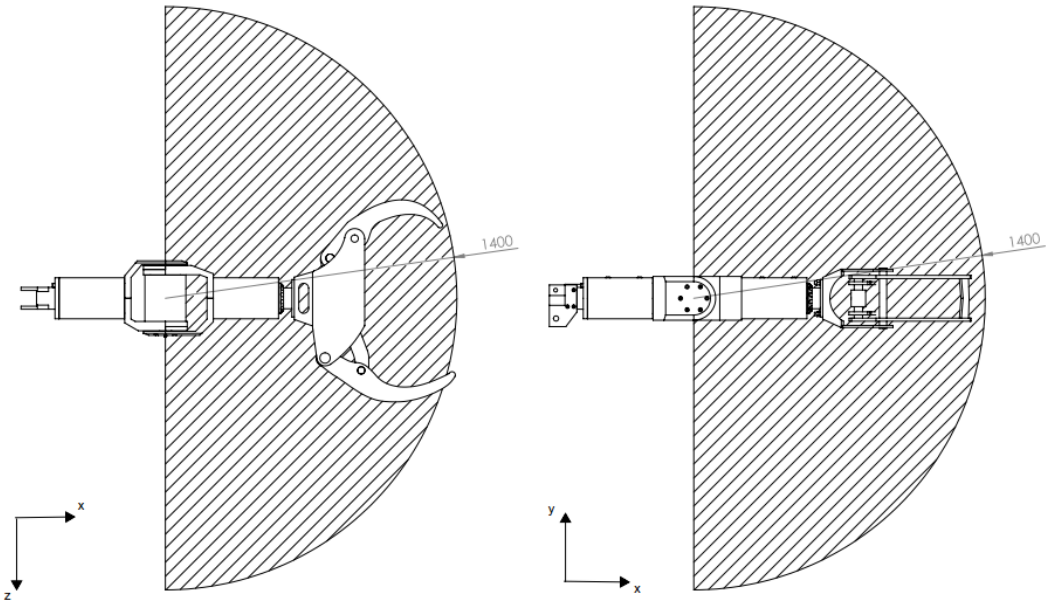

Figure 22. *Spherical wrist working envelope*

When connected to the HIAB loader crane, a full spherical work envelope for the six DoF manipulator is achieved. This means that the manipulator can move its end-effector, which in this case is the B15 grapple, to any point inside the envelope. Working envelopes are used to determine the workspaces of the manipulator. Working envelope also provides information about a safe distance, where an object can be located safely without a chance of collision with the manipulator.

5.1.2 Encoders

In closed-loop controlled systems, the position of the actuators are measured to enable control of the system, based on the difference between the required and measured values. In the underwater manipulator system, the angles of joints are measured and converted into Cartesian motions and forces of the manipulator. Calculated difference is used to control the actuators, in this case, the proportional valves connected to actuators.

The manipulator is designed to be equipped with rotary encoders attached to the joints

of the manipulator. Rotary encoders convert joint shaft rotation to output voltage signal which is translated to rotation angle within the control system.

The manipulator is equipped with Posital fraba IXARC UNS-ICD00 incremental encoders presented in figure 23. Encoders were chosen because they are IP68 class housing protected. IP codes are reviewed in section 2.2. Encoders are attached to the joints using flexible couplings. These couplings are required so that possible aligning or non-central rotation errors do not load the encoder shaft which only has limited axial and radial load capacity.

Figure 23. *Posital fraba IXARC UNS-ICD00 incremental rotary encoder [19]*

Posital Fraba UNS-ICD00 is an incremental encoder which means that it can only measure relative rotation. Encoders must be reset every time the control system is rebooted and the reset position has to be fixed in order to obtain relative data to that position. Control system is manually given information about current joint parameters as an input value so it can compare it to the encoder data.

Encoders used in the manipulator have a resolution of 16384 PPR or pulses per revolution. With a counter that counts rising and falling pulses, the resolution can be multiplied by four. With the connected counter, the Fraba encoder can measure angular differences as small as 0.0055 degrees.

UNS-ICD00 is IP68 class protected. It means that the encoder housing is dust-proof and dust is not allowed to penetrate the housing. Also the device can be submerged underwater and has to able stay waterproof for any given time. IPX8 test has to replicate the actual conditions that the housing is facing when continuously immersed.

Addition to the standard IP68 protection, Fraba is provided with IP69K protection. This protection class is defined in standard SFS-EN 60529 amendment A2 [20]. The additional protection class states that the encoder housing can withstand high pressure, high temperature water jets from any direction. This kind of protection is useful in applications where

regular washing of components is required, for example in food industry.

5.1.3 Bearings

To increase the stability and robustness of the manipulator structure, a symmetrical joint design is considered. Symmetrical design provides even load distribution across the joint structure.

Because the actuators of the spherical wrist don't have connecting interface on both ends of the actuator, the interface has to be designed and manufactured. Axis are constructed to the most outer links of joint 6.

Because the designed axis and connected housing do not rotate in same direction, bearings are required between the links. Deep groove ball bearings are chosen. Ball bearings don't require pretension which cannot be provided with the current joint design. In addition, deep groove ball bearing doesn't require to be installed in pairs compared to roller bearings, for example. Deep groove ball bearings can be installed independently to applications where only one bearing is required. The joint 6 of the manipulator is considered to be similar application because of the link design.

Two bearings are required for the design. First bearing is installed in the link 5 and another in link 6. Figure 24 is a cross-section of the joint 6 with bearings highlighted with red color for better visualization.

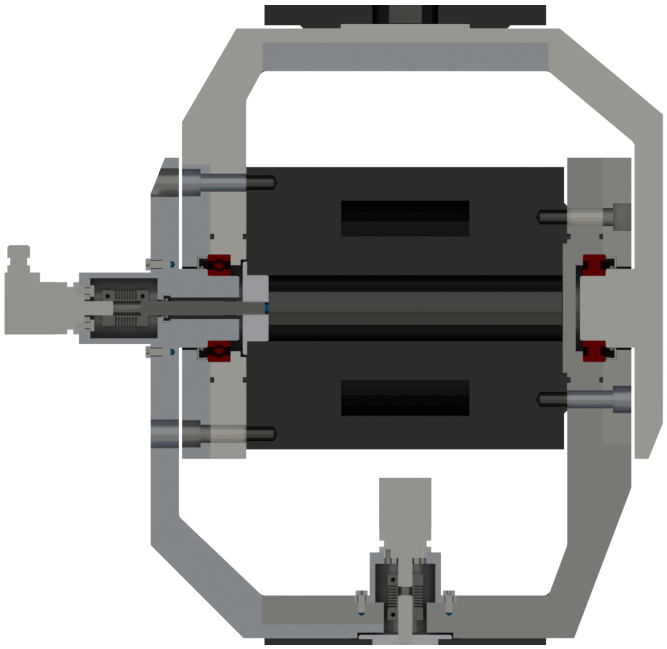

Figure 24. *Cross-section of the manipulator joint 6 with highlighted bearings*

Some of the deep groove ball bearings can withstand both axial and radial loads. In

manipulator application radial load is significant compared to axial. Axial loads are still present in the manipulator and that is why bearings that can withstand axial load are chosen. SKF 6009 was chosen for joint bearings. Loads in the joint are considered to be same on both sides of the actuator so identical bearings are used on both sides of the joint. Table 5 reviews the chosen bearing and the properties required for the structural design of the joint.

Table 5. *SKF 6009 deep groove ball bearing properties*

Parameter	**SKF 6009**
Outer diameter	75*mm*
Inner diameter	45*mm*
Width	16*mm*
Static load rating	14600*N*
Dynamic load rating	22100*N*
Mass	0,243*kg*

In the spherical wrist joints, actuator velocities are considered insignificant in the bearing calculation. Bearings are manufactured to withstand velocities of thousands of rounds per minute and based on the initial properties of the spherical wrist, maximum speed is in the range of 5 to 10 *rpm*. That is why static load rating is considered to be the significant factor in bearing calculation.

Static load rating describes the bearings ability to withstand static forces in the structure. These forces are calculated based on the worst case load scenario of the manipulator in which the load affecting the bearings are calculated based on the maximum output forces of the actuators. Worst case load scenario calculation is included in Appendix C.

The bearings were also chosen based on the physical properties of it. Width of a bearing was considered important for optimization reason. The width of the joint was minimized in order to prevent additional torque requirement for the actuators. Bearings are installed inside the link and the width of the bearing affects the size of the link structure significantly.

5.1.4 Sealing the structure

In mechanical design, sealing elements are used to create waterproof structure. Especially in hydraulic applications, sealing the structure and components is considered to be very significant design aspect.

Problem with using external seals, especially axial shaft seals, is that in dynamic applications sealing element causes additional friction between surfaces which affects the performance of the structure. The increased friction and reduction in performance has to be taken into account, if accurate calculation of the output power is required for the manipulator.

Underwater manipulator requires the structure to be waterproof. Some of the components, especially bearings are not corrosion resistant and sealing of bearings is required to prevent corrosion. Bearings are also lubricated using grease and seals are installed to prevent the mixation to external water to that grease which would affect the bearing lubrication and therefore the operation of the bearing.

Sealed and stainless steel bearings are available in the market and these alternatives were considered for the underwater manipulator. Bearings with sealed housing are not as well available as without seals. That is why external seals were used in the design. Seals are available in large variety of types and sizes.

Two types of seals were used, axial shaft seals and radial seals. Both of the seals are manufactured from nitrile rubber (NBR). Axial shaft seals are used inside the joint where dynamic surfaces are present. Sealing elements are chosen to withstand hydrostatic pressure. Axial seals able to withstand pressure up to $10bar$ are chosen. That way the $100m$ depth requirement can be achieved. In manipulator joint structure axial sealing elements are located next to bearing as well as around encoder shaft on both sides of the actuator. Axial sealing element locations can be observed in figure 25 in which sealing elements are highlighted in red color for visualization purposes.

Figure 25. *Sealing elements used in manipulator joint 6*

O-rings are used in static locations. As can be observed in figure 25, the joint structure has multiple paths where small amount of external water can leak to the bearings. In order to prevent this, o-ring grooves are machined into link.

5.2 Material evaluation

Material for the spherical wrist was chosen in the concept design phase of the project in order to validate initial structural calculations for the manipulator. Material properties such as Young's modulus, Poisson's ratio and yield strength were required to accurately calculate structural behaviour of the wrist.

Comparison was carried out between titanium, stainless steel and aluminium alloys. All of these possess great structural strength depending on alloy and above all, great corrosion resistance. These materials are used in commercial underwater manipulators as well, which was the reason for the decision.

Most important properties in the structural design point of view are elastic or Young's modulus, yield strength and density of the material. Young's modulus describes the stress-strain relation of the material. Under heavy load, materials tend to strain, which might cause inaccuracies in the operation of the system. The higher the elastic modulus is; more load or stress is required for the material to strain.

Yield strength describes the stress point after which plastic deformation occurs. The material cannot recover from plastic deformation which causes permanent deformation for the system.

In manipulator design, density was considered important property of the material, because it has direct affect to the weight of the manipulator. Increase in mass causes reduction in maximum payload capacity.

One alloy of each material is presented with the focus on mechanical properties of each material. Chosen material is presented as well as comparison chart between materials in the matter of the most significant design properties.

5.2.1 Titanium alloys

Titanium alloys are used primarily as the construction material in applications where high strength and low density is required, for example in aircraft, medical and spacecraft applications [21].

Most common titanium alloy used is Ti-6Al-4V. It is composed of 6% aluminium, 4% of vanadium, maximum of 0.25% iron, maximum of 0.2% oxygen and the rest (89.55%) being titanium. Alloy possesses great strength-to-weight ratio compared to steel and aluminium alloys considered for the manipulator. Structural and mechanical properties of Ti-6Al-4V are presented in table 6.

Table 6. *Structural and mechanical properties of Titanium alloy Ti-6Al-4V [22]*

Properties	**Ti-6Al-4V**
Yield strength	830 MPa
Tensile strength	900 MPa
Elastic modulus	113.8 GPa
Shear modulus	44 GPa
Poisson's ratio	0.342
Density	4430 kg/m^3

Yield point or yield strength of titanium alloy Ti-6Ai-4V is 830MPa which is far superior compared to aluminium and stainless steel alloys considered. However, in the concept design phase, maximum stress in the structure was calculated to be in the range from 150MPa to 200MPa with titanium alloy, so the material was considered to be abundant for the application.

Reason why titanium alloys are not widely used in number of applications other than those mentioned is the availability of the material. Pure and alloyed titanium is expensive compared to aluminium alloys, which are used widely in variety of structural applications. Another reason is poor machinability of the material. Poor machinability is caused by titanium's low thermal conductivity, high chemical reactivity and low elastic modulus [21]. High cutting temperatures are required with titanium. This results in short tool life expectancy. A variety of studies have been made to improve the machinability of the alloy by finding the right combination of cutting tool material, choosing the right machine tool and tooling parameters for the material [21].

5.2.2 Stainless steel

Another alternative for the material of the underwater manipulator was stainless steel. Stainless steel has great corrosion resistance with high mechanical and structural properties. High elastic modulus prevents deformation of the material even when under high stress. Stainless steel is a steel alloy with a minimum of 10.5% copper content. Copper gives the alloy its corrosion resistance properties by producing a passive protective layer of chromium oxide on the surface of the alloy. Passive layer means that the oxide film is self-renewable over short period of time, which prevents the alloy from corroding.

Stainless steels can be divided into three main categories based on the microstructure of the alloy. Different categories possess different properties in terms of ductility, corrosion resistance, and machinability. These properties are important when deciding the material for the spherical wrist. Stainless steel microstructure categories are presented in table 7.

Table 7. *Stainless steel microstructure comparison [23]*

Class	Ductility	Corrosion resistance	Machinability
Austenitic	high	high	medium
Ferritic	medium	medium	high
Martensitic	high	medium	low

In addition to microstructures listed in table 7, combinations are also available, for example very common combination of microstructures is Duplex steel. Duplex steel has a mixed microstructure of austenitic and ferritic steels. Duplex has superior strength properties compared to austenitic steel but reduced corrosion resistance due to the ferritic steel content. However, Duplex steel have great resistance against localized corrosion, such as pitting.

High availability of the steel makes it a widely used alternative in number of applications ranging from consumer products to oil and gas industry to chemical process industry. The most common product form of the stainless steel is cold rolled sheet [23].

Stainless steel has the highest density of the three materials considered for the manipulator. High density results in high mass of the structure. In robotic applications, mass of the structure is critical because it affects directly the maximum payload capacity.

Stainless steel alloy 1.4401 (AISI 316) was considered for the spherical wrist based on its structural properties and availability in general. Alloy 1.4401 possess high corrosion resistance and sufficient strength properties for the underwater spherical wrist. Based on the concept design of the spherical wrist, the machinable shape of the structure affects the availability of the material and therefore price of the material.

5.2.3 Aluminium alloys

Compared to stainless steel or titanium, aluminium alloys provide much lighter alternative with similar strength characteristics depending on the alloy. That is why aluminium alloys were considered as the construction material for the spherical wrist.

Aluminium alloys are divided into categories based on the main element that the aluminium is alloyed with. These categories are defined in standard SFS-EN 573-1 [24]. Table 8 represents the division of alloys based on the main alloying element. Every element provides different kind of characteristics for the alloy which is why different alloys are considered the best solution for particular applications. For example, Alloy EN AW 7075 is widely used in aircraft industry because of its superior strength properties com-

pared to other alloys. Its strength is compared to many steel alloys but because of its density, which is roughly one third the density of steel, the stress to density ratio is far more superior. Alloy 6082 on the other hand has inferior strength properties compared to 7075, but has superior corrosion resistance, which makes it more suitable choice for underwater applications. Both of these alloys were considered as the construction material in the initial design phase of the spherical wrist.

Table 8. *Aluminium alloy groups*

Alloy group	Alloying element
1xxx	Aluminium 99,00 % and greater
2xxx	Copper (Cu)
3xxx	Manganese (Mn)
4xxx	Silicon (Si)
5xxx	Magnesium (Mg)
6xxx	Magnesium (Mg) and silicon (Si)
7xxx	Zinc (Zn)
8xxx	Other elements

Because the manipulator is designed to operate underwater, the material assessment has to take corrosion resistance into account. Aluminium alloys, in general, have great characteristics to underwater applications because of its natural oxide layer on the surface of the metal to prevent corrosion. The oxide layer is self-renewable within certain time period.

Because the manipulator is designed to function underwater for quite some time, the natural oxide layer is not considered sufficient enough. That is why some surface treatment is required. Anodization is considered as the surface treatment to increase the corrosion resistance. Anodization of aluminium is reviewed in section 5.2.4. Anodization adds another requirement for the wrist material. Initial definition of loads were calculated to determine the maximum stress for each component of the spherical wrist. Material was chosen based on this strength requirement in addition to requirements listed earlier.

Aluminium alloy EN AW 6082-T6 was chosen as the material for the spherical. Alloy 6082 is widely used as a construction material in applications, where high stresses are measured. Alloy 6082-T6 possess good machinability and corrosion resistance. Because EN AW 6082-T6 is more common than, for example, EN AW 7075-T6, it is also more cost-effective which was one of the requirements of the design. Alloy EN AW 6082-T6 has sufficient strength properties for the wrist. In table 9 a comparison between Aluminium alloys EN AW 7075-T6 and EN AW 6082-T6 is presented.

Aluminium was also compared to stainless steel and titanium alloys. Table 10 represents a comparison between EN AW 6082-T6 in addition to stainless steel alloy 1.4401 and

Table 9. *Mechanical properties of aluminium alloys in extruded from, t<100mm*

Alloy	**Density** kg/m^3	**Elastic modulus** GPa	**Yield strength** MPa	**Tensile strength** MPa
EN AW-6082	2700	70	240	310
EN AW-7075	2700	70	460	510

titanium alloy Ti-6Al-4V, which were all considered for the spherical wrist.

Table 10. *Comparison between aluminium, stainless steel and titanium alloys, t<100mm*

Material	**Density** kg/m^3	**Elastic modulus** GPa	**Yield strength** MPa	**Tensile strength** MPa
EN AW 6082-T6	2700	70	240	310
SS EN 1.4401	7850	210	260	570
Titanium Ti-6Al-4V	4430	113.8	830	900

Even though both stainless steel and titanium alloys have superior strength properties to EN AW 6082-T6, the availability, weight and the cost of the material were the significant factors in this comparison. Because of the limited payload capacity of the HIAB loader crane, the spherical wrist made out of stainless steel would have lowered the payload of the whole underwater manipulator.

5.2.4 Anodization

Even though aluminium is corrosion resistant to some extent, it still requires a surface treatment in the underwater manipulator application. The time that aluminium alloy can be exposed to water is only limited without proper surface coating. That is why anodization of the aluminium is carried out for the spherical wrist.

Some aluminium alloys are more suitable for anodization than others. Standard SFS-EN ISO 7599 [25] states that if the copper content of the aluminium alloy exceeds 3.0%, coating will offer only limited protection for the alloy. Alloy EN AW 6082-T6 chosen for the manipulator has copper content maximum of 0.10% so it doesn't have effect on the anodization process.

Anodization of aluminium creates thick oxide layer on the surface of the alloy. The natural oxide layer is approximately 4 to 10nm thick [26] on the surface of an unanodized alloy and more than 25μm [25] when hard anodized or "hard-coated". With thicker oxide layer,

the corrosive material such as seawater is unable to penetrate through that layer to the aluminium. This ensures the corrosive resistance of the aluminium.

Article [27] explains the anodization process. In anodization process the aluminium part is exposed to an electrolyte, which is a specific chemical compound in liquid form. aluminium works as an anode when exposed to the electrolyte. A cathode of mild metal sheet is used in the process. The electrolyte differs depending on the anodization process and different electrolytes and cathodes provide different anodization results. When exposed to electric current, chemical reaction in the electrolyte results in a thick layer of metal oxide on the surface of the aluminium anode.

Anodization coatings are graded based on the thickness of the resulting oxide layer [25]. Thinnest layer anodization is merely decorative anodization which does affect the corrosion properties but not significantly. Thinnest layer anodization is used where the decorative surface and visual properties of the end result are the most important properties of the anodization. The thickest layer anodization is called hard anodization or "hard-coating". Hard-coating results in thick oxide film that improves corrosion resistance significantly while also increasing mechanical properties such as surface hardness.

5.3 Mechanical structure

After the decision for the symmetrical concept design was made, the actual design of the spherical wrist was carried out. Spherical wrist consists of the last four links of the underwater manipulator, links 4 through 7. The design began from the middle joint, joint 6, being the most demanding in terms of complexity of the structure. Joint 6 attaches links 5 and 6 together.

After the design of joint 6, the interface for the end-effector tooling was designed. Finally the design of link 4, to enable the attachment of the spherical wrist to the loader crane.

Following sections review these links in terms of detailed design, chosen components as well as solutions to each design problem and requirements described in previous sections. Exploded view of each link is provided. The design process was carried out using SolidWorks 2013.

5.3.1 Link 4

Link 4 is connecting link between the HIAB loader crane and the spherical wrist. Link consists of the joint actuator, Eckart E3 rotary actuator, and an interface for the loader

crane and the actuator.

Figure 26 is an exploded view of the link 4. all the components of the links are detached from each other and drawn out to visualize the positions and relations between the parts.

Figure 26. *Exploded view of the link 4*

The connecting interface is built from three pieces of aluminium attached together using bolted connection. The base of link 4 has a machined slot in the middle of the structure to enable the installation of rotary encoder inside the structure. Rotary encoder is attached to the actuator using flexible coupling and manufactured axis fitted in the feed-through hole of the actuator.

5.3.2 Link 5

Joint 6 being the most crucial part of the wrist design, links 5 and 6 around that particular joint were the main concern during the design phase. These links contain the most complex structure of the wrist. Figure 27 is an exploded view of the link 5.

The designed link consists of two L-shaped parts attached to each other and secured with a plate pressing the parts to previous joint, i.e. Eckart E3 actuator. These main parts of the links are each machined from a solid piece of aluminium to create stiff structure. Bolted connections were also considered but during structural validation, the stress was calculated to be redundant for the connection to withstand maximum load.

The size of the joint was kept as small as possible to retain the torque requirement as low as possible. Increase in size increases the torque lever which would cause additional load for the structure.

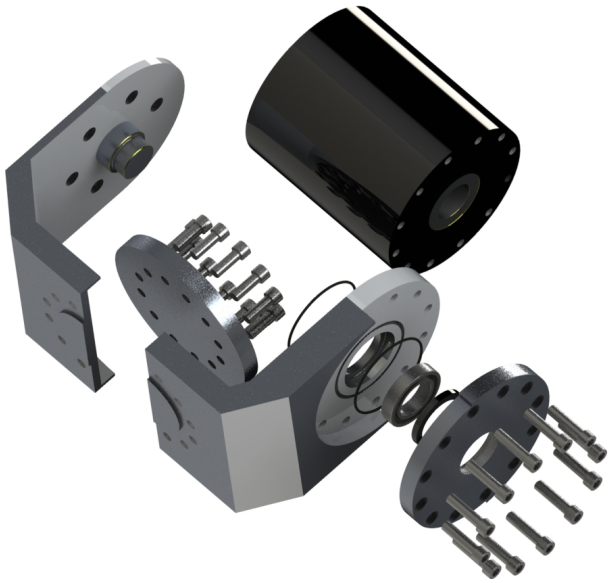

Figure 27. *Exploded view of link 5*

In addition to the structural parts of the link, additional components, such as, bearing and seals are required. The bearing is required for the next link to be attached to the joint axis. Symmetrical revolute joint is created using this connection. Because the structure has to be waterproof, the bearing must be sealed inside the structure. Axial seals and o-rings are used to prevent contact with surrounding seawater.

5.3.3 Link 6

Link 6 consists of the second part of joint 6. The mechanical structure of the link is very similar to link 5 for the reason of symmetrical design approach. Additional components such as encoder, bearing and seals are also added to the structure. Figure 28 represents the exploded view of the link.

Encoders required for joints 6 and 7 are both included in link 6 structure. Both encoders are attached to the rotary actuator by flexible coupling. Couplings provide stability and flexibility in case of misalignment of axes.

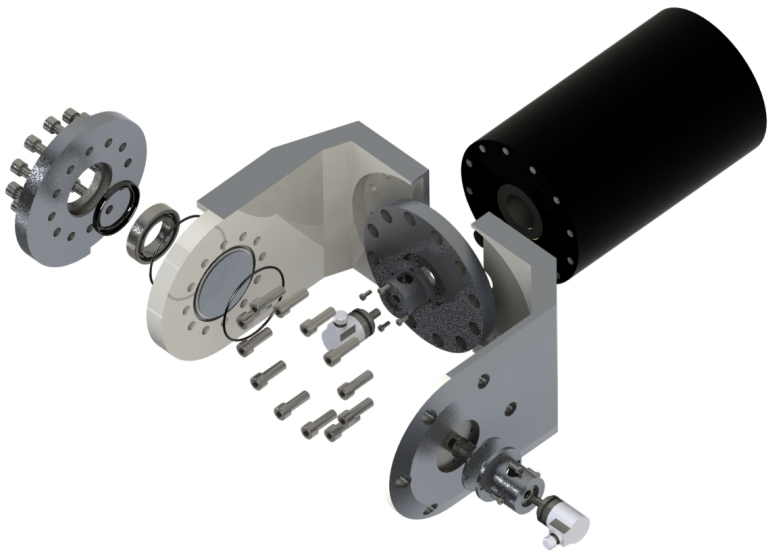

Figure 28. *Exploded view of link 6*

For possible maintenance purposes, both links, 5 and 6, are designed so that the joint 6 Eckart E3 actuator can be detached from the structure without disassembling the whole structure. One L-part can be detached from both of the links and joint actuator can be removed. This enables possibility to remove the actuator, while the spherical wrist is attached to the underwater manipulator. The structure can still withstand static load of the wrist.

5.3.4 Link 7

Final link of the underwater manipulator is link 7. Link 7 is an interface between the joint 7 rotary actuator and end-effector tool, Vahva B15 grapple. Figure 29 presents the exploded view of the link. Vahva grapple is also included in figure to visualize the connection of the end-effector.

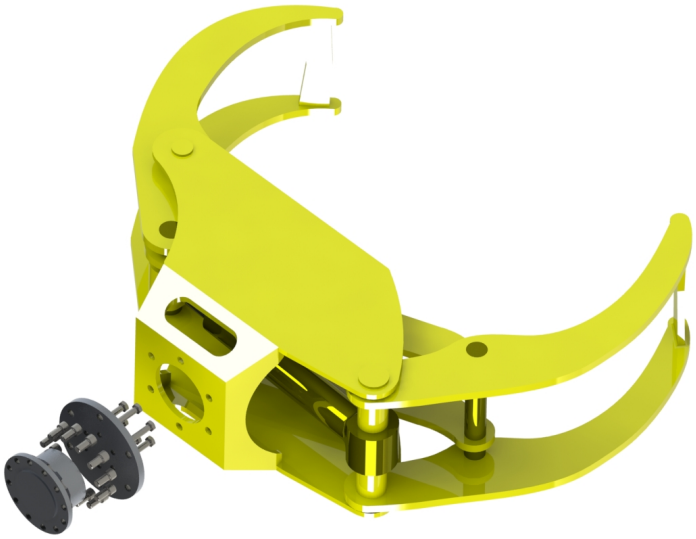

Figure 29. *Exploded view of link 7 with the end-effector tooling Vahva B15*

Link is constructed from two pieces of aluminium. First part is attached to the actuator and the second part to the grapple. The rotation angle of the joint is measured in link 6 structure, where the encoder is attached to the feed-through hole of the actuator. Final rendering of the complete underwater manipulator is included in Appendix A.

5.4 Hydraulic system

The hydraulic system for the underwater manipulator consists of external power unit, actuators, directional valves and hoses. Hydraulic oil is used as a medium in the system. Oil is pumped to the system from the centralized power unit located in the IHA heavy lab. That is why pumps or additional components, such as filtration, is not included in the hydraulic system of the manipulator. Hydraulic diagram of the underwater manipulator is presented in Appendix D.

Waterproof components are required for the hydraulic system. Corrosion resistant fittings are used. Directional valves are designed to be installed inside a waterproof case that can be submerged with the manipulator. Valve casing and modification of hydraulic system is reviewed in section 7.2.3.

Because the actuators of the spherical wrist are commercial components, hydraulics for the actuators are designed to be connected using external hoses. Feed-throughs for the actuators and link structure would have been time and resource consuming, and irrelevant considering the purpose of the design being only a tool for the control system and research.

Maximum required flow for the spherical wrist is calculated using the maximum velocity of the joints. For the spherical wrist, the Eckart E3 are considered to perform full circle of motion in 5 seconds. From the data sheet of the actuator, for one degree of rotation, $3.371 cm^3$ of oil is required which result in approximately $15 l/min$ flow to the actuator for maximum velocity. Maximum working pressure of the Eckart actuators is $210 bar$.

The hydraulic system of the whole underwater manipulator is designed so that the control system can be enabled for each joint of the manipulator. The manipulator consists of 7 hydraulically powered joints, as well as the hydraulic grapple. Each joint is attached to Bosch Rexroth 4/3 proportional directional valve. List of components used in the hydraulic system is also included in Appendix D.

Valves are connected to control system, which control each joint separately. Open control, closed loop control as well as Cartesian control is implemented to the manipulator.

6. STRUCTURAL VALIDATION OF THE SPHERICAL WRIST

Solid material can only withstand finite amount of load without breaking or deforming. To prevent structures from breaking, material has to be chosen and structure has to be designed to withstand loads applied in both static and dynamic scenarios [28].

In order to fully understand the behaviour of the mechanism, calculations are required for the structure. Structural validation is carried out by calculating stresses and displacements for the structure under load. Finite Element Method (FEM) is utilized for this calculation. In this chapter, FEM is described and applied to the spherical wrist.

FEM is made possible by the improvements in computing power [28]. Vast amount of softwares are developed to use FEM in the structural calculation. In this design process, SolidWorks Simulation is used for the FEM calculation. Solidworks Simulation is an add-in of the SolidWorks CAD software, which was used to model the spherical wrist.

6.1 Finite Element Method

If no external load is applied, the structure is in equilibrium. After external load is applied, the structure applies loads within to prevent deformation and to stay in equilibrium. These loads within the structure cause stress to the structure. Load causes stress and stress causes strain to the material. To calculate stress and strain parameters for the structure, FEM can be applied. FEM, like numerical methods in general, are about creating finite amount of algebraic equations to describe the system and providing solution based on the variables within those equations [29].

FEM is about dividing the structure to smaller finite elements and creating numerical equation to each element to calculate stress and strain within the structure. The division of the structure is called meshing. Meshing creates approximation of the actual structure that depends on the intensity of the mesh i.e. size of the finite elements.

Finite elements are connected to each other by nodes. FEM calculation is based on the calculation of values in each node and applying those results to connecting nodes using already calculated values. That way whole structure can be validated and stress and strain

values can be presented in each node.

After meshing the structure, material properties of the structure are taken into account before solving the algebraic equations. Stiffness matrix $k^{(e)}$ is applied for each connection point or node of the element. Stiffness matrix depends on the mechanical properties and geometry of the element. For each element e the relation between displacement and force according to [29] can be written as:

$$\mathbf{q}^{(e)} = \mathbf{K}^{(e)}\mathbf{a}^{(e)} \tag{3}$$

Where:

- $\mathbf{q}^{(e)}$ Element nodal equilibrating force vector
- $\mathbf{K}^{(e)}$ Combined stiffness matrix of the element
- $\mathbf{a}^{(e)}$ Element nodal displacement vector

For the whole structure the equation (3) can be written as follows:

$$\mathbf{Ka} = \mathbf{f} \tag{4}$$

Where:

- $\mathbf{K}$ Global stiffness matrix
- $\mathbf{a}$ Global displacement vector
- $\mathbf{f}$ Global load vector

$\mathbf{f}$ is the external load vector applied to the system. Only unknown variable in the equation (4) is the global displacement vector $\mathbf{a}$. After solving this, displacement vector $\mathbf{a}^{(e)}$ for each element can be calculated. When nodal displacements are known, nodal force vector $\mathbf{q}^{(e)}$ can be constructed. Nodal force vector represents the internal forces of each node in the element.

Strain vector of each element is calculated using equation 5:

$$\varepsilon = \mathbf{Ba}^{(e)} \tag{5}$$

Where:

- ε strain vector
- $\mathbf{B}$ Element strain matrix

After strain of each element is calculated, the stress within the element can be obtained. For this, constitutive matrix $\mathbf{D}$ is required. Matrix $\mathbf{D}$ combines the material-specific parameters of the structure. These material-specific parameters are Young's modulus and

Poisson's ratio. The matrix can be expressed as follows:

$$\mathbf{D} = \frac{E}{(1+\upsilon)(1-2\upsilon)} \begin{bmatrix} 1-\upsilon & \upsilon & \upsilon & 0 & 0 & 0 \\ \upsilon & 1-\upsilon & \upsilon & 0 & 0 & 0 \\ \upsilon & \upsilon & 1-\upsilon & 0 & 0 & 0 \\ 0 & 0 & 0 & \frac{1}{2}-\upsilon & 0 & 0 \\ 0 & 0 & 0 & 0 & \frac{1}{2}-\upsilon & 0 \\ 0 & 0 & 0 & 0 & 0 & \frac{1}{2}-\upsilon \end{bmatrix} \tag{6}$$

Where:

E Young's modulus of the material
υ Poisson's ratio of the material

The stress within component depends on the external loads, component geometry (size and cross-sectional area of the component) and component material. Stress matrix includes all the normal stresses and shear stresses of the element. Stress matrix can be calculated by combining equations (5) and (6) in the form of equation (7)

$$\sigma = \mathbf{D}\varepsilon \tag{7}$$

Where:

σ stress matrix of the element

In FEM, stresses are presented in von Mises stress. Von Mises stress is the combination of shear and normal stresses and can be calculated using equation (8). Von Mises stress is applicable when ductile materials, such as metals, and their plastic deformation is studied [28].

$$\sigma_v = \sqrt{\frac{1}{2}[(\sigma_x-\sigma_y)^2+(\sigma_y-\sigma_z)^2+(\sigma_z-\sigma_x)^2+6({\tau_{xy}}^2+{\tau_{yz}}^2+{\tau_{xz}}^2)]} \tag{8}$$

Where:

σ_v Von Mises stress of the element
$\sigma_{x,y,z}$ Normal stress
$\tau_{xy,yz,xz}$ Shear stress

Calculated von Mises stress is compared to the material-specific yield criterion which is the maximum stress the material can withstand before permanent deforming. With brittle materials, this criterion means that the material starts to break after exceeding the point. Yield criterion is also called yield strength and is labelled ($R_{p0.2}$) in the literature.

6.1.1 Factor of Safety

To ensure endurance of the designed structure, a Factor of Safety (FoS) is determined in the requirements phase of the design process. This factor determines how much more stress the system can endure before plastic deformation occurs. In machine design, the FoS is usually between 1.5 and 2 based on application. It means that the system can withstand 1.5 to 2 times more than the maximum stress calculated before exceeding the yield strength of the material.

$$\sigma_v \leq \frac{R_{p0.2}}{FoS} \tag{9}$$

Where:

$R_{p0.2}$	Yield strength of the material
FoS	Factor of Safety

In the spherical wrist design process, minimum FoS of 1.5 is determined. That means that because the construction material EN AW 6082-T6 has a yield strength of $240MPa$, the maximum von Mises stress in any case should not exceed $160MPa$. The same FoS is applied to every component in the spherical wrist.

6.2 Worst case load

To use FEM calculation in structural validation of the spherical wrist, the external load has to be calculated prior to applying FEM. With stationary structures, determining external load would be straightforward because only acceleration affecting the structure would be the gravitational acceleration g. External load would be the mass of the payload times the gravitational acceleration.

In the spherical wrist case, the maximum external load is much higher than the gravitational force of the payload. That is because the acceleration of the manipulator is variable when the manipulator is moving. Variable acceleration affects the force at the end of the manipulator which results in variable loading force.

Because the lift cylinder of the HIAB limits maximum payload of the loader crane, the cylinder force is determined to be the most affecting in terms of the end-effector load. The lift cylinder acts on the joint 2 labelled in section 4.1. For the manipulator to stay in equilibrium, there has to be same quantity of reaction force opposing the cylinder force. This reaction force is determined to be sum of the masses of the manipulator from joint 1 to the end-effector and an external force higher than the actual payload. Maximum force from the lift cylinder is determined using the predetermined pressure limit of the actuator.

The pressure limit is controlled with the pressure valves located to each directional control valve in valve block.

Because joint 2 is fixed, the masses and payload of the manipulator create torque to that joint. Torque from lift cylinder and torque from the loads cancel each other out to achieve equilibrium. Because the manipulator is not a straight beam, the torque lever of joint 2 doesn't necessarily go through the manipulator structure. An algorithm is created in the calculation phase to maximize the payload at the end-effector to determine the worst case load scenario. Calculation of the worst case load scenario is presented in Appendix C. Worst case scenario is the case, where the actuators of the manipulator have the maximum force output at the same time. This case determines the maximum force at the end-effector.

Because the manipulator is operated in six dimensional space, the worst case load has to be determined in this space respectively. Coordinate frame is attached to the end-effector in an orientation presented in figure 30.

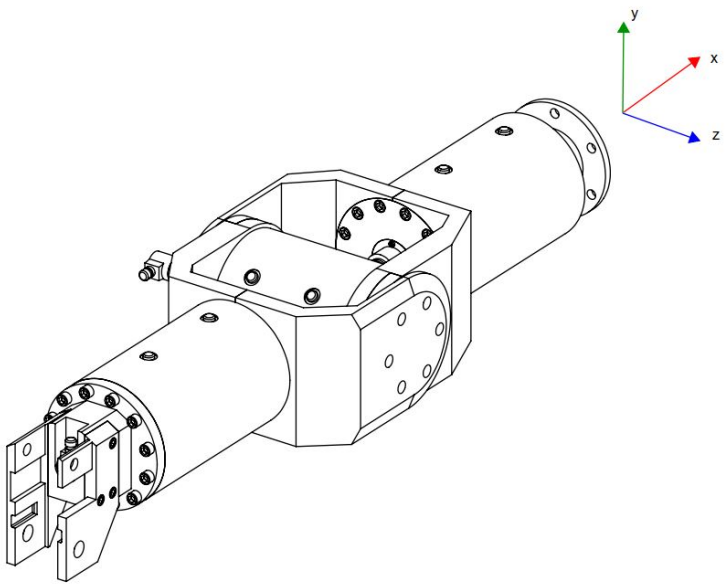

Figure 30. *Coordinate frame attached to the spherical wrist*

Lift cylinder force described earlier gives the load of directions x and y to the end-effector. Force in z direction is calculated using same principle but the cylinder in question is the base cylinder of the crane responsible of the turning motion for the crane. Cylinder produces torque to the base revolute joint which is converted as a force at the end-effector using correct torque lever. End-effector load in Cartesian space is presented in table 11 divided by the direction of the force to the end-effector.

Table 11. *Forces to the end-effector of manipulator*

Direction	**Force** [N]
x	-2700
y	-4400
z	-1200

6.3 Structural analysis results

The following sections review the result of the finite element analysis. As already mentioned, FEM is applied using Solidwork's Simulation add-in. Links 4 through 7 are analysed, because links 1 through 3 form the HIAB loader crane which cannot be structurally validated because of insufficient data of the structure. Maximum von Mises stress, maximum displacement and FoS are presented for each link in the following sections. Minimum FoS requirement of 1.5 is used in the calculation.

FEM is carried out by applying loads from worst case load calculation, Appendix C, to one end of each link and fixing the other end on its place. This way structurally balanced link as achieved. Material for the spherical wrist is chosen as aluminium alloy 6082-T6. Solidworks library, however, does not have this particular material included. Because significant material properties are Poisson's ratio, elastic modulus and yield strength, aluminium alloy with similar properties is considered for the structural analysis. Aluminium alloy 6063-T83 is chosen from the material library with same material properties as with alloy 6082-T6.

6.3.1 Link 7

Link 7 is the end-effector of the whole manipulator. Grapple Vahva B15 and payload are connected to link and considered one mass object. Link 7 could have been attached to actuator Eckart E3, because of the link being merely an adapter between the actuator and the grapple. However, when considering the adapter part as its own link, the division of structure, defined in section 5.3, is followed which is why the adapter is considered as its own link.

Figure 31 represents the meshed structure of the link. Structure is stabilized using fixtures on one end of the link and calculated worst case load forces are applied on the other end. Constraints are placed on the interface of link 7 which is attached to the rotary actuator. Model is meshed as a one rigid part to ensure correct distribution of calculated stress from

applied load all the way to applied fixtures.

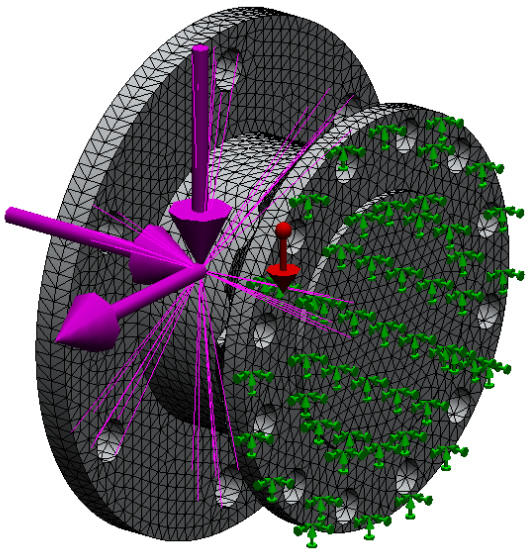

Figure 31. *Meshed model of link 7 with constraints and applied loads*

Solidworks simulation calculates the von Mises stress and displacements in the structure using the FEM. Simulation results of maximum stress can be observed in figure 32.

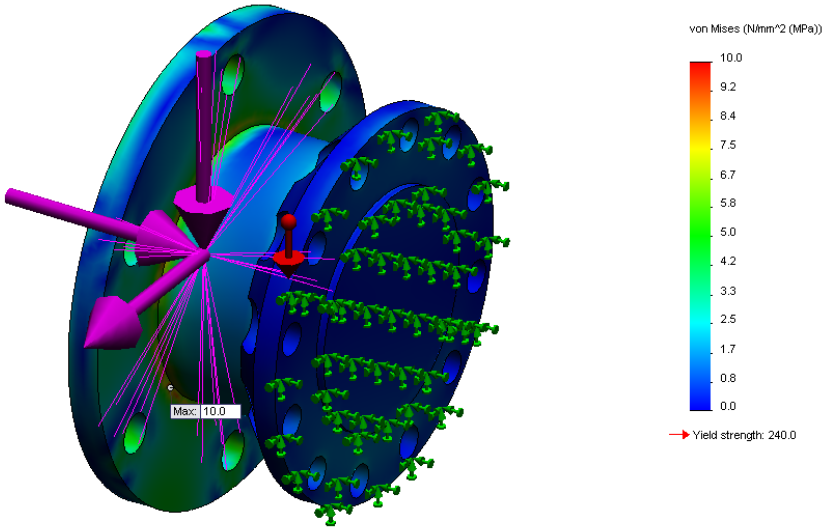

Figure 32. *Stress distribution of link 7*

Maximum stress of 10.0MPa is calculated which is sufficiently low for the structure to hold under worst case load. FoS calculation is performed to visually validate the relation between maximum stress and the yield strength of the material according to equation 9. Results are presented in figure 33.

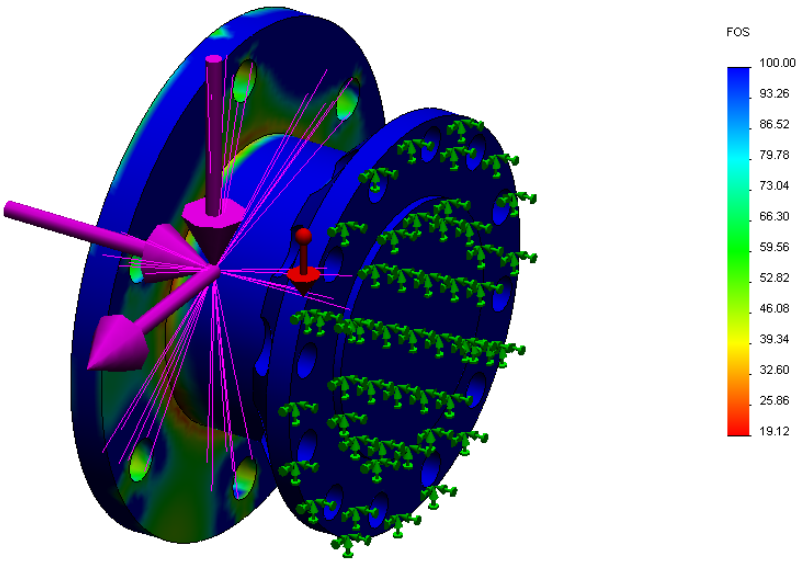

Figure 33. *FoS for link 7*

As can be observed from the figure, minimum FoS is 19.12. That means that the structure can hold more than 19 times the maximum stress applied before permanent deformation occurs. FoS visualization was limited to 100.0 so that regions under maximum stress can be easily observed from the structure.

Maximum displacements are calculated for each link of the spherical wrist. Deformation of structure affects the accuracy of the manipulator. Deformation is minimized by choosing stiff material and designing the structure so that it doesn't deform under load. Maximum displacements of link 7 can be observed in figure 34.

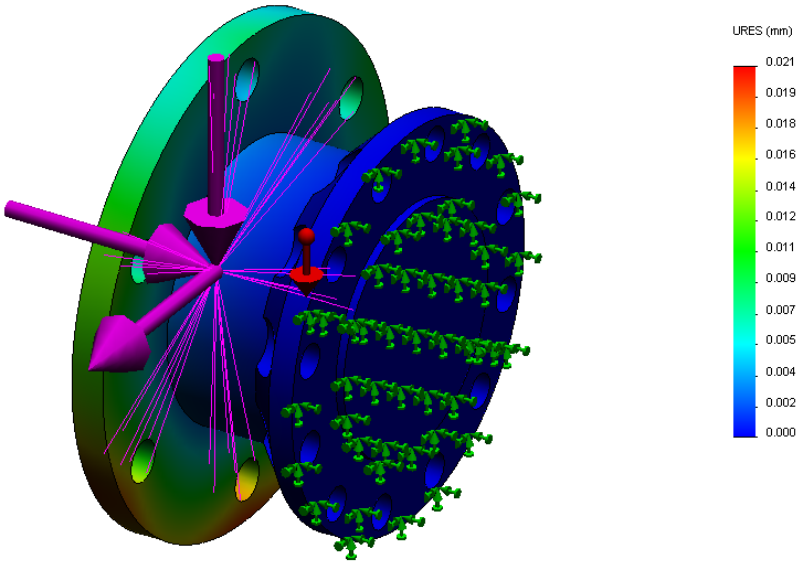

Figure 34. *Maximum displacement of link 7*

Maximum deformation of 0.021*mm* is calculated. The displacement presented is resultant value which does not take into account the direction of deformation. With hydraulic manipulator, where compressibility of the medium affects the accuracy of the structure significantly, deformation in range of fraction of a millimetre is considered more than sufficient in structural validation.

6.3.2 Link 6

Link 6 is the pitch arm of the spherical wrist. Link 6 consists of the second rotary actuator and the second part of the middle joint. Bearings, seals and encoders are suppressed from the model during analysis. These components are crucial part in term of functionality of the link but not in terms of structural analysis and the affect in results is insignificant. Meshed model of link 6 is presented in figure 35.

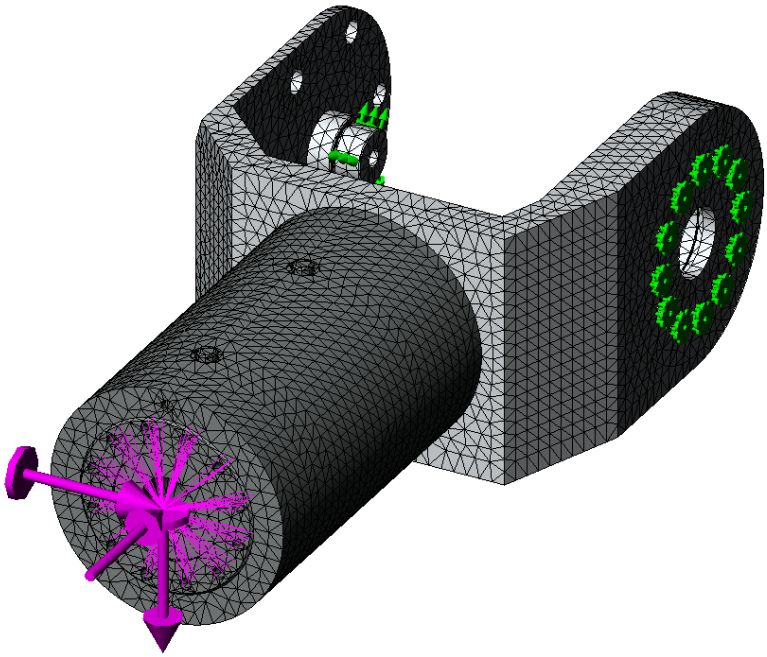

Figure 35. *Meshed model of link 6 with constraints and applied loads*

Fixtures of the link are applied on the interface where connecting bolts are attached to connect the linkage to previous rotary actuator. Also fixed hinge is applied on the bearing axis to demonstrate the rotation of bearing axis under a load. Loads applied are the resultant forces from link 7. Loads are applied at the end of the third rotary actuator, which is also the connecting interface between links 6 and 7. Stress results for link 6 are presented in figure 36.

Maximum stress calculated for the link is $43.9MPa$. Stress region is located on the connecting interface between the joint structure and the actuator. This maximum stress is quite low which means that the structure can easily withstand maximum load applied. FoS is calculated using the maximum stress and yield strength of the material. Visualized results of the calculation is presented in figure 37 with minimum FoS being 3.09. Value is sufficient compared to required FoS of 1.5.

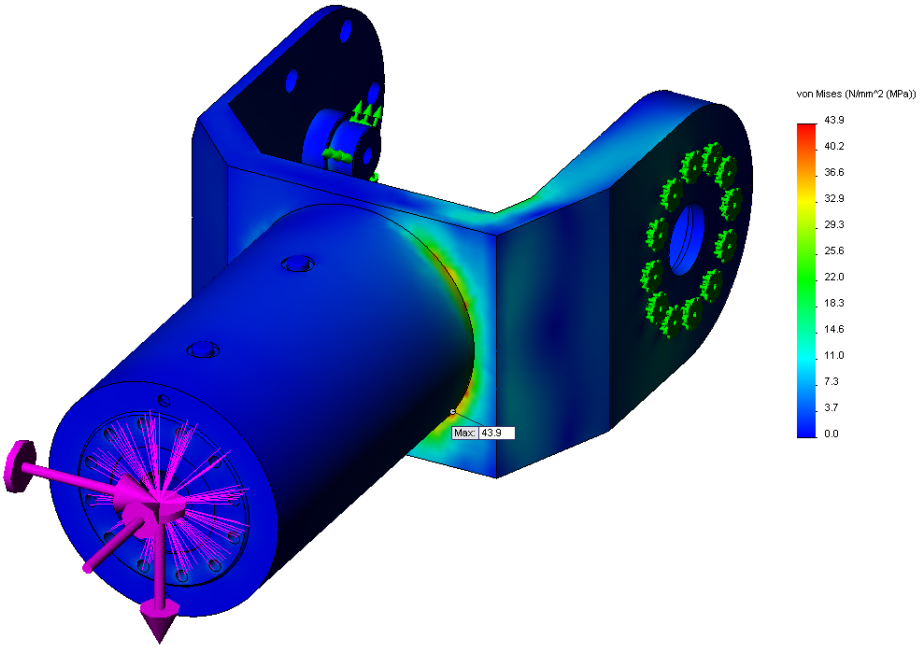

Figure 36. *Stress distribution of link 6*

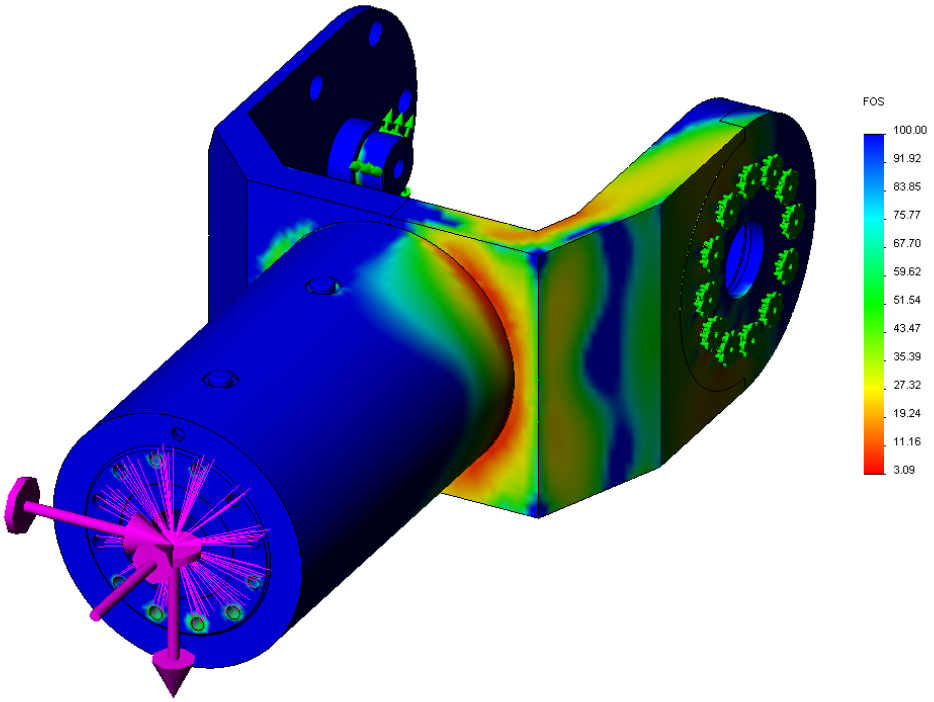

Figure 37. *FoS for link 6*

Long structure of the link affects significantly on the deformation of the structure. Applied force affects one end of the link and with resulting torque, the structure deforms resulting in large displacements especially if the stiffness of the material is insufficient. Deformation of the link 6 is presented in figure 38.

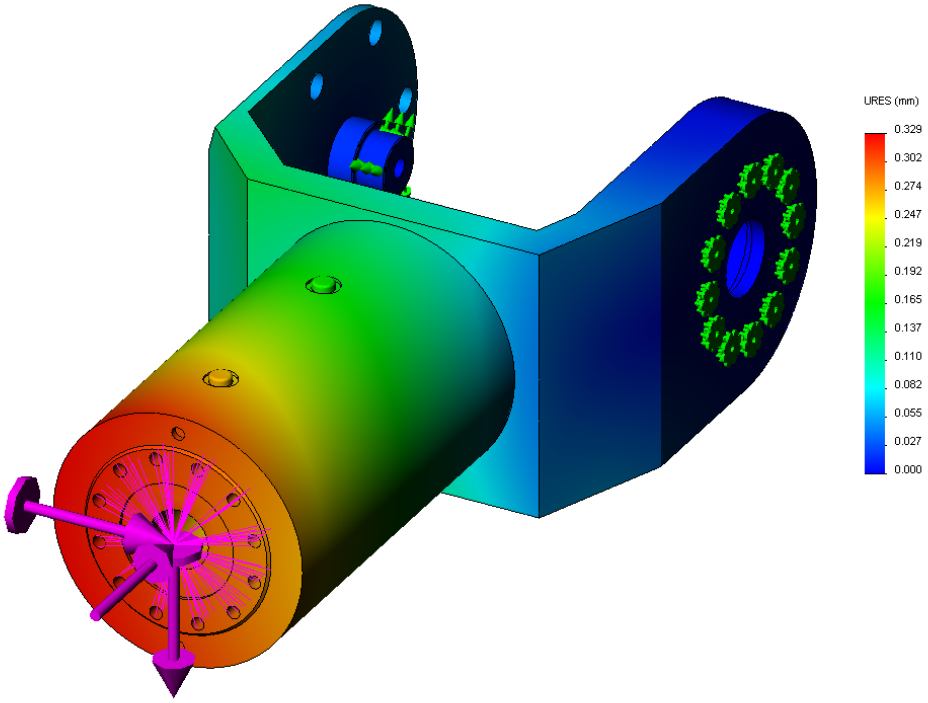

Figure 38. *Maximum displacement of link 6*

Maximum deformation of 0.329*mm* was calculated. value is still sufficient even though it is 14 times higher than with link 7.

6.3.3 Link 5

Link 5 is the first part of the middle joint, joint 6 of the manipulator. The structure of the link is relatively short because the actuator is perpendicular compared to two other rotary actuators.

Loads are applied on the bearing axis in joint structure as well as the bearing housing wall on the other side of the joint. With this kind of load distribution, applied load is divided as evenly as possible to both sides of the link. Loads applied are the resultant forces from link 6. Fixtures are applied on end of the joint, where link 4 rotary actuator is connected. Figure 39 represents the meshed model of link 5 with applied loads and constraints.

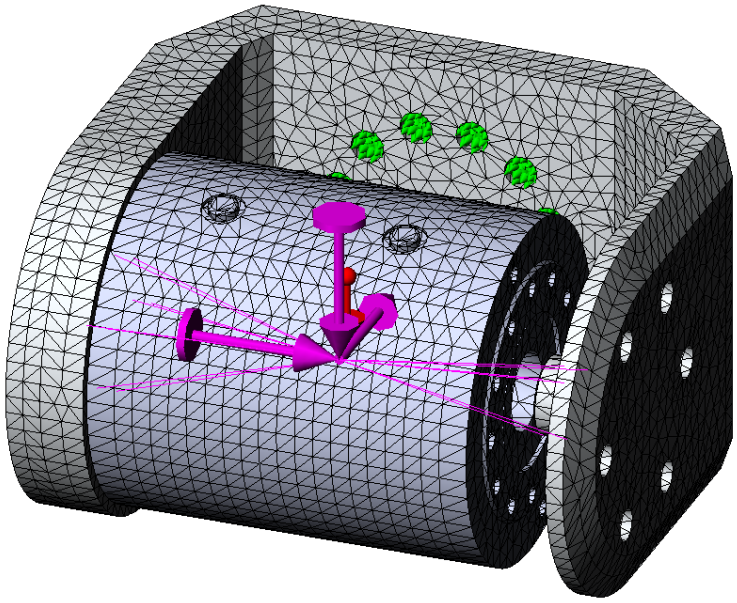

Figure 39. *Meshed model of link 5 with constraints and applied loads*

Maximum stress calculation is applied on the model. Addition to loads, the mass of the rotary actuator applies on the joint structure creating maximum stress on the side where the actuator is attached. Maximum stress distribution can be observed in figure 40.

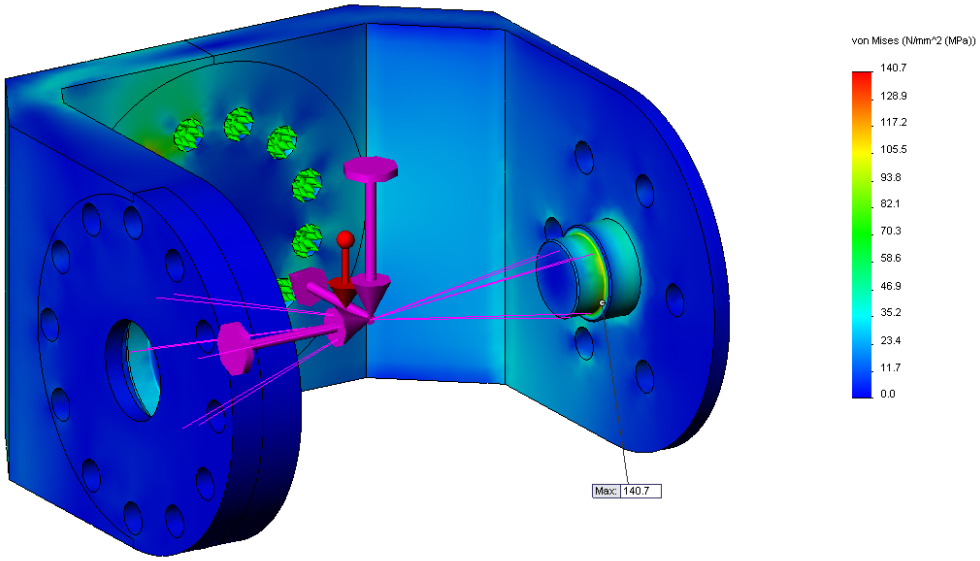

Figure 40. *Stress distribution of link 5*

Maximum stress of 140.7*MPa* is calculated. This is relatively high compared to previous stress calculations. However, the material yield strength being 240*MPa* with the chosen aluminium alloy 6082-T6, the structure can still withstand the applied load, as can be observed in figure 41.

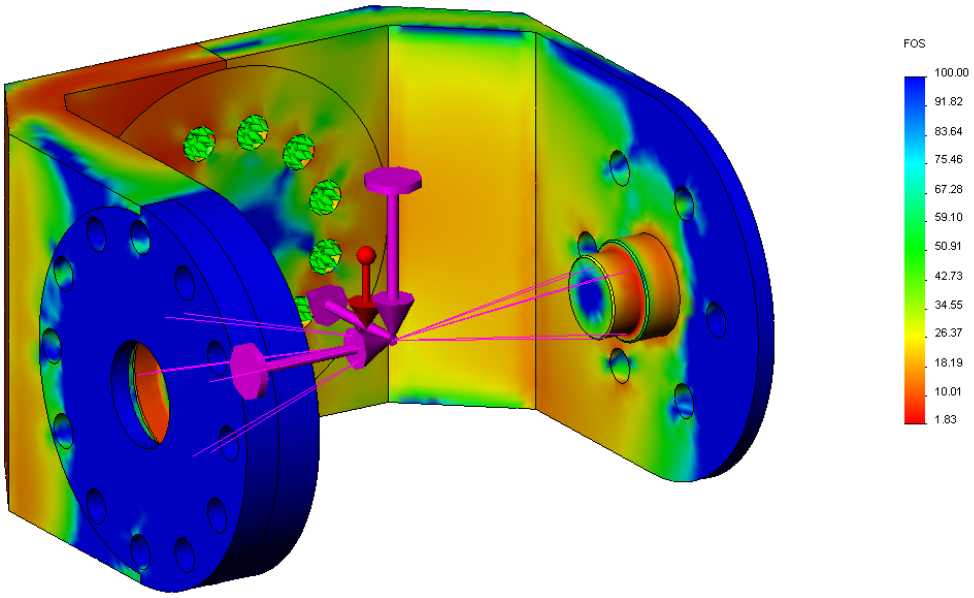

Figure 41. *FoS for link 5*

Calculated minimum FoS of 1.83 is higher than the required value of 1.5. That means that the structure is strong enough and doesn't deform permanently when under maximum load. Maximum displacement of the link structure was calculated and the simulated model with results are presented in figure 42.

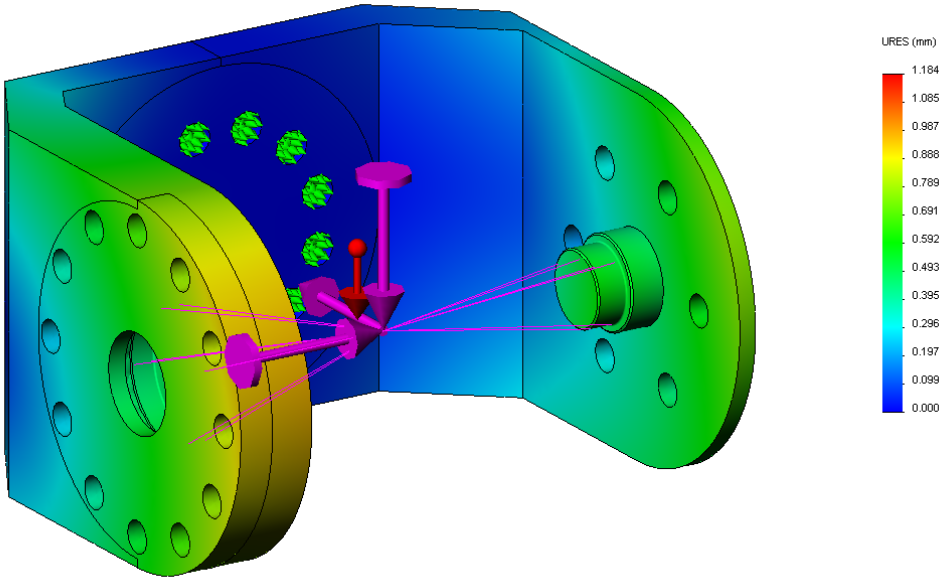

Figure 42. *Maximum displacement of link 5*

Maximum displacement of the structure is located on the end of the rotary actuator. In real scenario, the result may vary due to the fact that the second part of the middle joint is connected to the rotary actuator of link 5. The second part keeps the rotary actuator aligned with the bearing axis which result in smaller displacements. In the simulated model maximum resultant displacement of 1.184*mm* is calculated which is relatively high compared to previous links but still low enough for hydraulic manipulator where large cylinders with flexible hoses are present. Large cylinder chambers and flexible hoses introduce large bulk modulus to the system which results in overall flexible structure.

6.3.4 Link 4

Last part of the structural validation is the connecting link between the designed 3 DoF spherical wrist and the HIAB loader crane. Link 4 consists of the first rotary actuator of the spherical wrist and the connector parts for the HIAB loader crane. Meshed model of link 4 is presented in figure 43.

Loads are applied on the end of the rotary actuator respectively to previous link, link 5, where fixtures were applied on the corresponding interface. Surface interacting with the loader crane is considered fixed in addition to holes where connecting axis are installed. Finite element analysis results for the stress distribution are presented in figure 44 with corresponding colors of red for the highest stress and blue for the lowest stress.

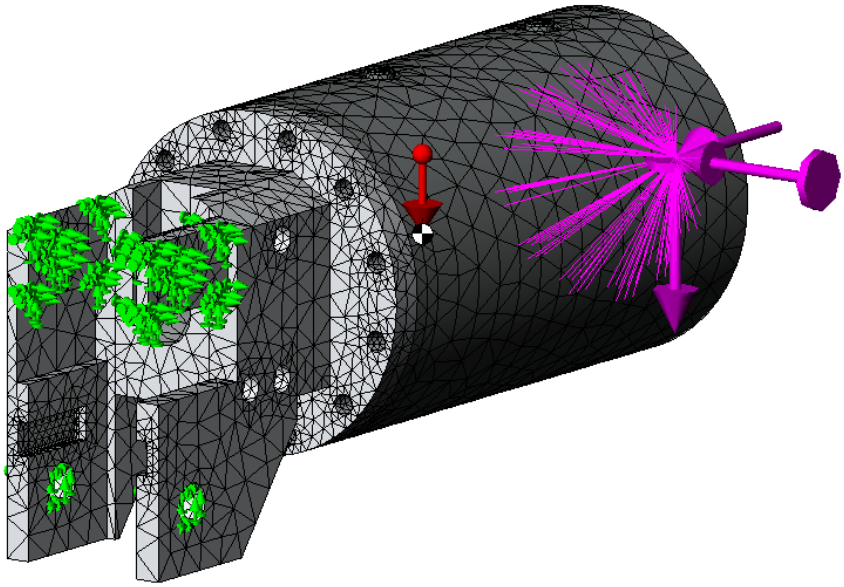

Figure 43. *Meshed model of link 4 with constraints and applied loads*

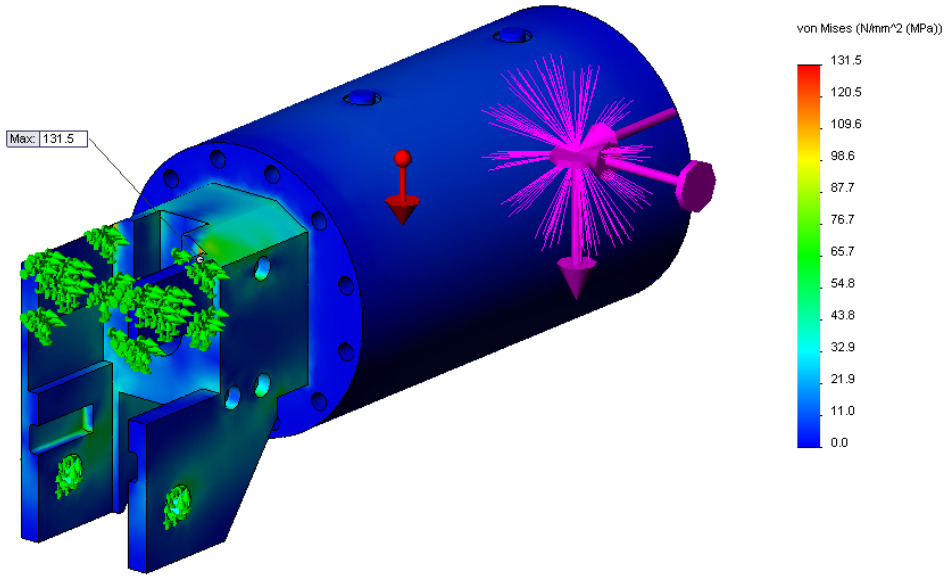

Figure 44. *Stress distribution of link 4*

Maximum stress of 131.5MPa is calculated. With material yield strength of 240MPa the maximum stress is more than sufficient for the structure to hold under worst case load scenario. FoS's are presented in figure 45 with limited maximum FoS of 100.0 for visualization purposes.

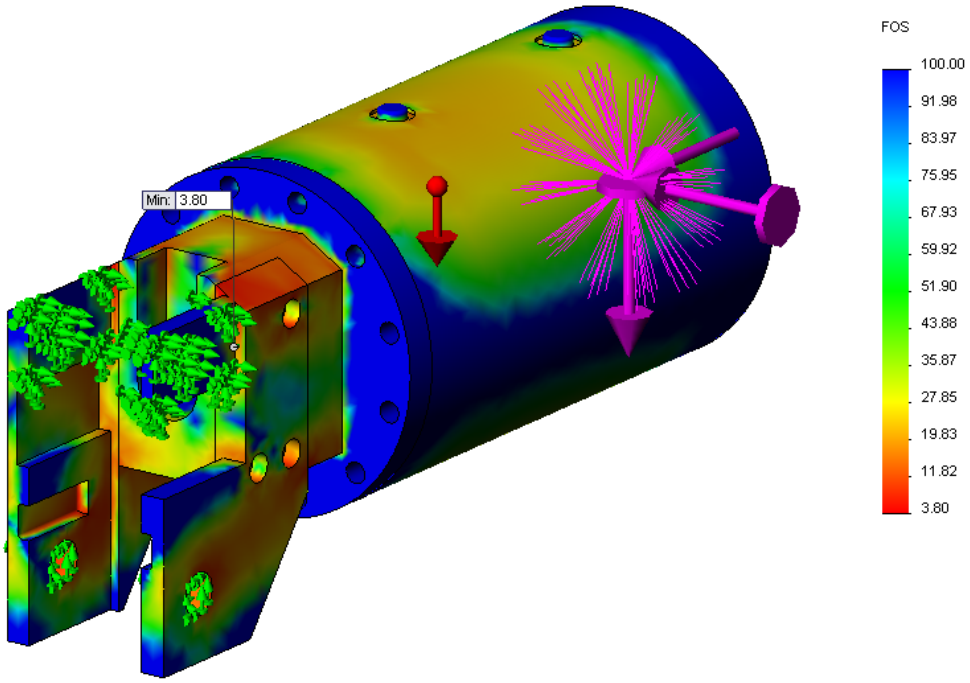

Figure 45. *FoS for link 4*

Deformation of the link structure is presented in figure 46 with maximum displacement of 0.509*mm*. With structure this large, the deformation is considered sufficiently low for the manipulator structure.

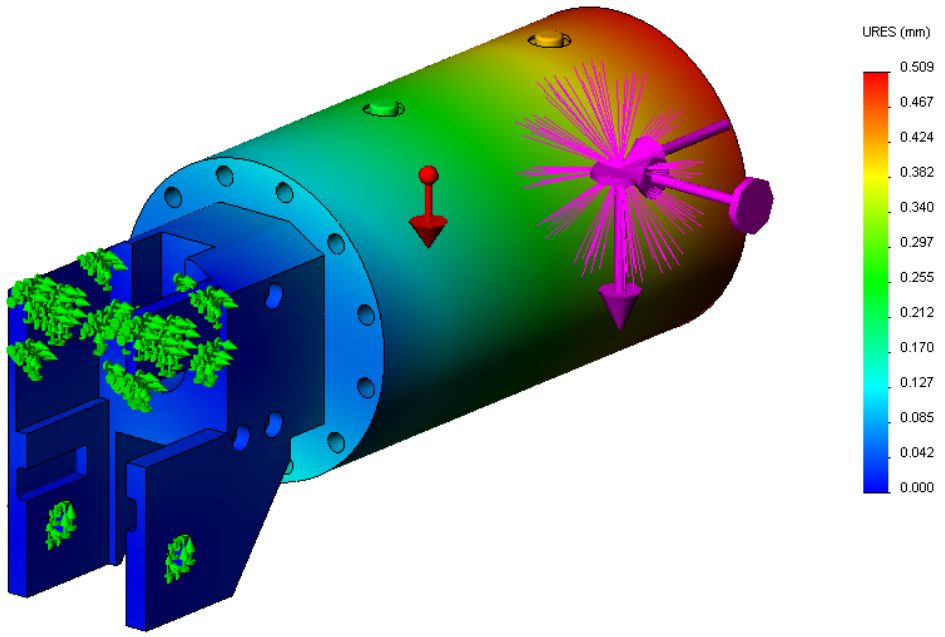

Figure 46. *Maximum displacement of link 4*

After the structural validation of the 3 DoF spherical wrist, the results are analysed and de-

termined that the structure is rigid enough to withstand the worst case load scenario with the chosen material of aluminium alloy 6082-T6. All of the components in the manipulator can withstand the loads caused by the maximum payload and dynamic movement causing variable acceleration for the structure.

7. REQUIRED MANIPULATOR MODIFICATIONS FOR SUBMERGING

The underwater manipulator design consists mostly of COTS (Commercial Off-The-Shelf) components. These components are not custom-made to be able to withstand subsea conditions. 3 DoF spherical wrist can be designed waterproof from the start, but the COTS parts of the manipulators have to be evaluated and possibly modified to enable underwater operation. List of required modifications and aspects taken into account in the modification process is provided in this chapter.

Even though manipulator is designed and modified to operate in subsea environments, the testing itself will be carried out in a water tank located in the TUT campus. Testing doesn't provide complete environmental aspects of the real environment but main features such as water drag effect in control of the manipulator can be tested. Tests are designed to be carried out in cycle of hours, when the manipulator is submerged.

7.1 Test environment

To test underwater operation of the designed manipulator, manipulator will be submerged. IHA has a water tank in its heavy lab on the university campus. The tank is 5 times 6 metres in cross-section dimensions and a depth of 10 metres.

The medium in the test environment is seawater to fully simulate the real world test environment. Seawater contains large amount of sodium and chlorine, which together combine into sodium chloride, or salt. Sodium chloride is the source of the saltiness in seawater. Sodium chloride is also very corrosive substance when in contact with metals. Corrosion resistant materials are considered when sodium chloride is known to be present.

Manipulator is designed to be installed on the bottom of the tank on a pedestal. When tests are carried out, the tank is filled with water. After the tests are completed, the tank is drained. This way, the test environment simulates a real life situation in which the crawler is submerged only for a limited amount of time instead of permanently placing the manipulator underwater.

Before submerging, the manipulator has to be tested on the dry ground. A pedestal was

constructed on the ground floor of the heavy lab next to the water tank. The working envelope of the manipulator is limited both while on the dry ground and while submerged. The main functionalities of the manipulator can be tested and the control system implemented before submerging the manipulator.

Main focus of the testing is in the control of the manipulator and how a viscous water drag effect affects the performance of the manipulator. Control system implementation can be carried out on the dry ground and possible corrections and tunings to be made before submerging the manipulator. That way the possible errors in control are considered to be caused by submerging and changed environment.

7.2 HIAB 033 loader crane modification

Even though the HIAB loader crane is designed to be used outdoors, it is not completely waterproof. Number of modifications are required for the crane for underwater operation. Modifications for the loader crane provide waterproof and leak-proof system. Following sections provide description of the critical components and aspects which to modify focusing on materials, coatings and especially hydraulics.

7.2.1 Joints

Critical part of the HIAB loader crane in waterproof and corrosion resistance aspect are the joints of the crane. There are three structural joints and four cylinder joints in the crane that rotate according to control. All of these joints are exposed to ambient air and therefore to ambient water when submerged. Joints are already designed to withstand some amount of water because the crane is designed to be used outdoors.

To ensure proper movement of the joints, lubrication is taken into account. Joints are lubricated using grease. However, the grease applied at the factory might not possess the required water resistance properties. That is why the lubrication has to be changed to ensure proper lubrication and furthermore proper movement of the joints.

Next, special water resistant greases are compared and evaluated. Synthetic water-resistant grease, for example Neste OH grease [30] is waterproof and designed especially in applications, where frequent and prolonged contact with water is present. OH grease is designed especially for mobile working machine's joints. Proper lubrication creates a fluid film to prevent metal to metal contact as well as waterproof seal for the joint to prevent metal joint being exposed to external water and furthermore corroding the metal of the joint.

7.2.2 Materials

HIAB 033 loader crane's mechanical parts are manufactured from steel alloy and applied with a coat of paint. Accurate evaluation of the material is not possible due to insufficient data availability. The applied coating consists of pre-treatment of the material followed by powder coating, which results in corrosion resistant coating. The coating is called "nDurance" [31]. nDurance starts with application of chrome-free, nano-ceramic shield giving excellent corrosion resistance. Primer of lacquer polymer coating is applied after that. Primer increases the corrosion resistance even further and enables the application of powder coating on the surface of the metal.

HIAB loader crane can withstand submerged for a limited amount of time. Because the loader crane is designed to be used outdoors practically indefinitely, the materials can withstand contact to water for a short periods of time.

To prevent corrosion through the mechanical part's surface, the coating must be examined and possible cracks and holes shall be coated afterwards. If the surface is exposed to water through small crack, a possibility of localized pitting corrosion occurs in the part.

7.2.3 Valve pack/Hydraulics

In underwater hydraulic systems, the operating depth is important in terms of hydraulic system design. As stated in [32], in depths under 50 metres, the Hydraulic Power Unit (HPU) can be placed above sea level and only the actuators are submerged. Pipes and hoses required to transfer hydraulic medium underwater are subject to hydrostatic pressure, which has to be compensated in order to achieve maximum required power of the actuator. To compensate the hydrostatic pressure outside the hoses, adjustable back pressure valve is fitted in the return line. This valve ensures a higher pressure in the return line compared to ambient hydrostatic pressure.

In depths over 50 metres, HPU is often submerged with the actuator. HPU is installed inside the oil reservoir. The reservoir includes a pressure compensator which is an open piston mechanism that is pre-pressurized with a set of springs [32]. Bottom of the piston is subject to hydrostatic pressure which determines the pressure affecting the piston and thus, increasing the pressure inside the reservoir. Figure 47 represents the two concepts of the underwater hydraulic systems.

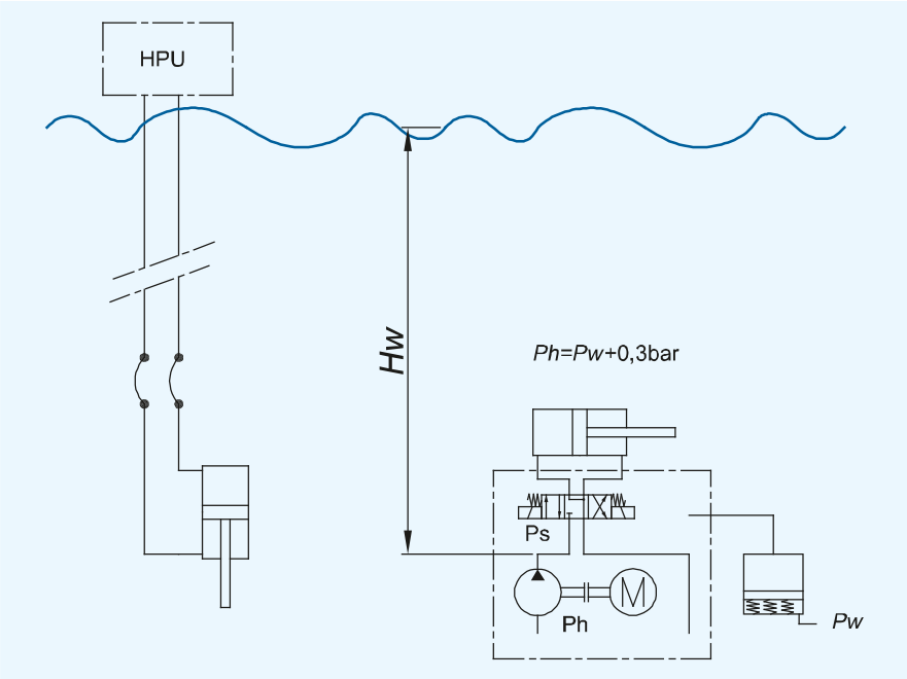

Figure 47. *Two hydraulic systems with HPU installed above and below water*

As stated in [32], in depths up to 50 metres, valve set is sometimes placed in a pressure resistant casing, which can withstand the external pressure. Valve casing is filled with oil and an external pressure compensator is installed with the casing. In the underwater manipulator system design, such approach is considered. Control valves of the underwater manipulator are designed to be lowered into the water tank with the manipulator. Therefore, a waterproof case is designed for the valves. Casing provides compact housing for the valves to ensure waterproof and leak-proof system.

Number of commercial applications for the valve systems are provided especially for hydraulic systems of ROV's. One example of a commercial valve pack is General function valve pack by Forum [33]. Valve pack is used in ROV tooling applications. Figure 48 represents the model of the valve pack.

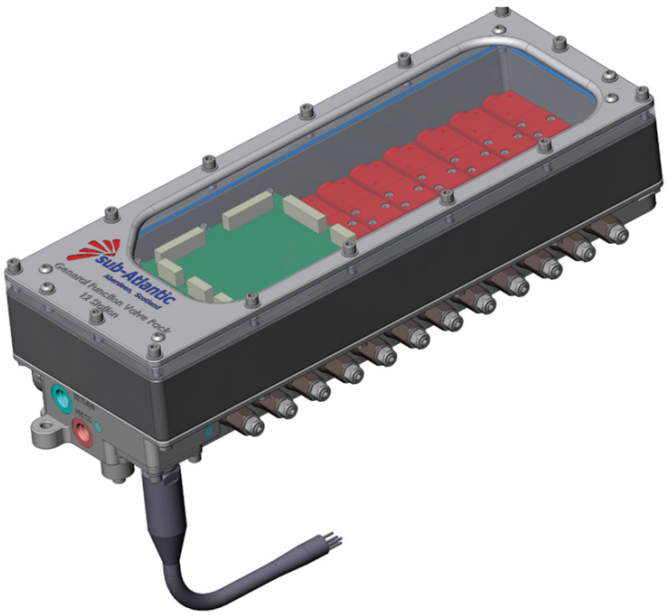

Figure 48. *General function valve pack by Forum*

Valve pack consists of control valves, pressure valves and control board for the valves [33]. Inputs and outputs of the pack include power, hydraulic oil pressure and tank lines as well as control signal. When valves are lowered with the manipulator, the amount of required cables and hoses are minimized.

Because the designed manipulator is already equipped with control valves, the approach is to design only a casing for the valves rather than acquire complete valve pack for the manipulator. The casing is designed to be constructed from 3 pieces of aluminium alloy 6082-T6, the same alloy that were used in the spherical wrist. Alloy is chosen because of its corrosion resistance properties and great availability as a construction material. Another approach would be to design the casing out of stainless steel. That way, the structure would be able to be manufactured from sheet metal and weld together. This approach would reduce the amount time required in machining. Also, no additional sealing would be required, if the welding can be assured to be waterproof. Figure 49 represents a model of the designed valve casing. The sides of the case are transparent for better visualization of the model.

Two concepts of the valve pack are reviewed. In first concept, the valve pack contains only the valves required while the control system is left on the surface. This requires individual control cable for each of the valves to be lowered to the valve pack. Pressure sensors of the actuators are also installed inside the case to enable usage of non-waterproof components. Figure 49 represents this concept. One advantage of the concept is that no additional control board is required inside the valve case. This results in minimized size of the casing itself. However, lowering individual control cables require more cable and connectors between the systems. More connectors increase the probability of leak in the

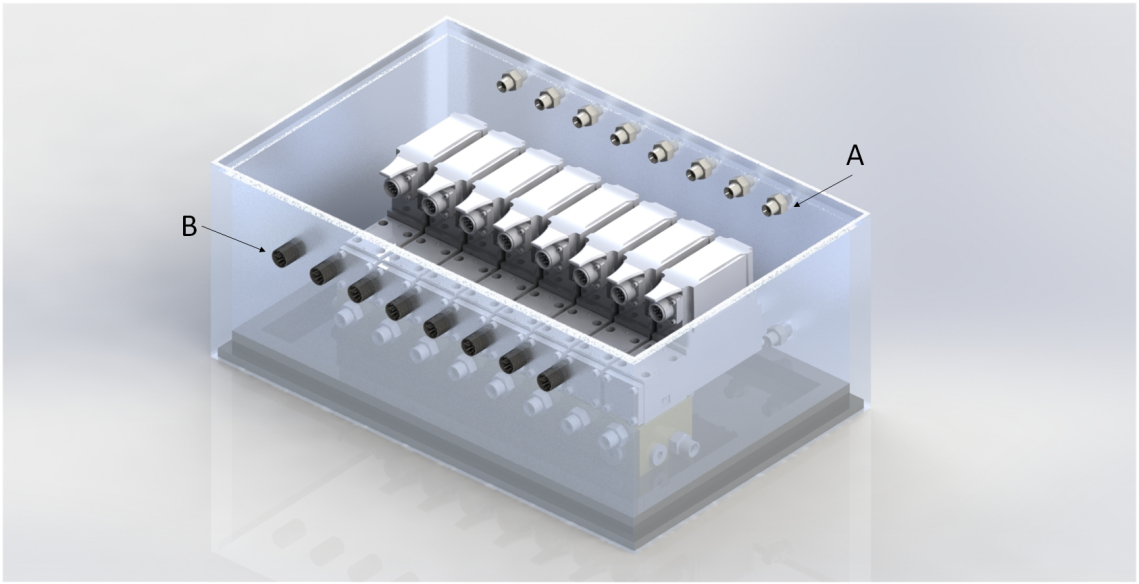

Figure 49. *Concept design of the underwater valve pack*

system.

Second concept has built in control board inside the valve case. The board is connected to the surface via single control cable using, for example, EtherCAT connection. Advantage with the second concept is the minimized amount of cables required from the surface. Only required cables are control signal from the surface control system as well as input voltage for the valves. The casing required however is larger and requires more space next to the manipulator because of the embedded control board needs to be inside the case.

Hydraulic connections of the casing are designed to be sealed. Sealed adapters are installed through the casing (labelled A in figure 49). Also electrical connection's sealing is taken into account. Special sealed electric connectors (labelled B in figure 49) are chosen in both cases of the casing concept. This results in waterproof valve casing for the underwater manipulator.

8. CONCLUSION

The purpose of the thesis project was to design a 6 DoF underwater manipulator. The manipulator is used as a tool for control system development in Seaspider research project.

The underwater manipulator is divided into two parts; the arm and the wrist. This is common practice in robotic manipulator applications. The arm is constructed from commercial HIAB loader crane. Commercial crane limits the design by introducing fixed payload capacity to the design prior to actual design process. That is why payload capacity of the underwater manipulator cannot be determined before concept design of the spherical wrist is completed.

The mechanical design of the 3 DoF spherical wrist, attached to the arm, is the most important part of the thesis project. The wrist was constructed from COTS actuators, Eckart E3 rotary actuators. Mechanical parts are modelled using SolidWorks CAD software. An aluminium chassis is designed for the spherical wrist. Aluminium is chosen based on the material evaluation. The most challenging part of the project was to design stiff mechanical parts from aluminium with limited yield strength.

After the design of the spherical wrist, the design was validated using FEM calculation. Some iteration was required based on the maximum stress occurring in the mechanical parts. SolidWorks Simulation is used in the structural analysis for the compatibility reason with the SolidWorks CAD software.

Underwater operation of the manipulator will be tested in IHA heavy lab in 10 meter deep water tank. Only limited operation can be evaluated in this water tank.

Before the manipulator is submerged, some modifications are required. The loader crane is not designed to be used underwater. Materials of the crane as well as lubrication of the joints are considered and modified to ensure proper operation underwater.

Hydraulics of the manipulator are designed to be submerged with the manipulator. That is why waterproof valve casing was designed and manufactured. Two concepts of the casing are reviewed; one with valve control system installed inside the case and another without.

To evaluate the completion of requirements, defined in the early phase of the design project (presented in section 3), a re-evaluation of the requirements is carried out. In table 12, status of the requirement is presented. The requirement can be either "ongoing"

or "completed". Ongoing requirement means, that the requirement might be designed into the system but is not yet evaluated due to the ongoing project. Completed requirement means, that the requirement have been designed into the system and it has been evaluated.

Table 12. *Evaluation of the underwater manipulator requirements*

Requirement	Type	Description	Status
Req01	functional	Minimum depth capacity of the underwater manipulator shall be 100m underwater	Completed
Req02	non-functional	The arm of the underwater manipulator shall be commercial loader crane	Completed
Req03	non-functional	The wrist of the underwater manipulator shall be 3 DoF spherical wrist	Completed
Req04	non-functional	The actuators of the spherical wrist shall be Eckart E3 hydraulic rotary actuators	Completed
Req05	non-functional	The underwater manipulator shall be corrosion resistant	Ongoing
Req06	non-functional	The payload capacity of the spherical wrist shall be maximized based on the torque output of the Eckart E3 hydraulic actuators	Completed
Req07	non-functional	Factor of Safety of 1.5 shall be used in structural validation	Completed
Req08	non-functional	The underwater manipulator shall be IP68 class protected	Completed

Ongoing requirements of the project are related to the waterproof and corrosion resistance of the structure. The manufacturing of the spherical wrist is not yet completed. After the manufacturing process, anodization is performed for the spherical wrist. This ensures the corrosion resistant structure and completes the requirement.

For future development, some modifications are considered. At the moment, hydraulic power is provided by external hoses to the manipulator. For future development, hydraulics can be constructed inside the mechanical links of the manipulator. Also changing the directional control valves to smaller servo valves (for example Moog servo valves) and installing those directly next to the actuator, the number of required hoses is minimized.

Based on the work cycle required with the manipulator, the end-effector tooling can be changed to reduce the mass of the tool significantly and furthermore increasing the pay-

load capacity of the manipulator. Aluminium or Titanium grapples should be considered and possibly designed because of the lower density and therefore lower weight with aluminium and lower weight and higher stiffness with titanium compared to the steel used in the grapple at the current application.

BIBLIOGRAPHY

[1] M. Siven, "Vedenalaisen Hydraulisen Puomin Rannemekanismin Suunnittelu", Master's thesis, Tampere University Of Technology, Finland, 2015.

[2] Academy of Finland. (2014). Arctic academy programme (arktiko), Programme description, [Online]. Available: http://www.aka.fi/en/research-and-science-policy/academy-programmes/current-programmes/arctic-academy-programme/ (visited on Jul. 14, 2016).

[3] J. Mattila, V. Kyrki, J. Koivumäki, and M. Suomalainen. (2015). Seaspider - cooperative heavy-duty hydraulic manipulators for sustainable subsea infrastructure installation and dismantling, Research poster, [Online]. Available: http://www.aka.fi/globalassets/32akatemiaohjelmat/arktinen/posterit_avajaisseminaari/poster_mattila_seaspider.pdf (visited on Jul. 13, 2016).

[4] SMD. (2013). Quasar ROV product page, [Online]. Available: http://smd.co.uk/products/work-class-rov-systems/quasar.htm (visited on Jul. 21, 2016).

[5] M. A. Jordán and J. L. Bustamante, "Numerical stability analysis and control of umbilical rov systems in one-degree-of-freedom taut–slack condition", *Nonlinear Dynamics*, vol. 49, no. 1, pp. 163–191, 2007.

[6] SMD. (2013). CBT1100 Trencher data sheet, [Online]. Available: http://smd.co.uk/download.php?file=/page/123_172_72.pdf (visited on Jul. 29, 2016).

[7] E. group. (2016). ECA group ARM 7E electrical manipulator data sheet, [Online]. Available: http://eca-media.ecagroup.com/player/pdf?key=c9faef88b70ef5dade8%20ffa5249ae5584 (visited on Aug. 30, 2016).

[8] R. D. Christ and R. L. Wernli, Sr., *The ROV manual*, 2nd ed. Oxford: Butterworth-Heinemann, 2014, 678 pp.

[9] Schilling robotics. (2014). Manipulator systems brochure, [Online]. Available: http://www.fmctechnologies.com/~/media/Schillingrobotics/Brochures/Manipulator-Brochure.ashx (visited on Sep. 1, 2016).

[10] SFS-EN 60529 + A1, "Degrees of protection provided by enclosures (IP code)", Finnish standards association SFS, Standard, 2000.

[11] E. Hull, K. Jackson, and J. Dick, *Requirements engineering*, 1st ed. Springer London, 2005, 198 pp.

[12] M. Steele, W. Ermold, and J. Zhang, "Arctic ocean surface warming trends over the past 100 years", *Geophysical Research Letters*, vol. 35, no. 2, p. 6, 2008.

[13] P. Valkama, "Design of six degree of freedom water hydraulic arm for remote handling", Master's thesis, Tampere University of Technology, 2008, 102 pp.

[14] Micromatic. (2016). SS rotary actuator product page, [Online]. Available: http://www.micromaticllc.com/product/ss1-ss130-end-mount (visited on Sep. 1, 2016).

[15] Eckart. (2007). Eckart E1 rotary actuator Data sheet, [Online]. Available: http://www.teittinen.fi/PDF-Esitteet/Eckart/E1_en.pdf (visited on Jul. 25, 2016).

[16] Koneenosapalvelu. (2016). VAHVA B15 hydraulic grapple product page, [Online]. Available: http://www.koneosapalvelu.com/en/b-models (visited on Jul. 11, 2016).

[17] Kuka robotics. (2016). Kuka KR 1000 Titan data sheet, [Online]. Available: http://www.kuka-robotics.com/res/sps/48ec812b-1b29-4789-8ac2-598aff70abc0_Spez_KR_1000_titan_PA_en.pdf (visited on Oct. 10, 2016).

[18] Eckart. (2007). Eckart E3 Data sheet, [Online]. Available: https://www.icfluid.com/PDF/Eckart-E3.pdf (visited on Jul. 15, 2016).

[19] Posital fraba. (2015). Posital fraba UCD-INS00 rotary encoder product page, [Online]. Available: https://www.posital.com/en/products/incremental-encoders/incremental-encoder-finder/UCD-INS0X-XXXX-D10D-ARW/112723201/detail.php (visited on Jul. 18, 2016).

[20] SFS-EN 60529/A2, "Degrees of protection provided by enclosures (IP code)", Finnish standards association SFS, Standard, 2013.

[21] J. P. Davim, Ed., *Machining of Titanium Alloys*, 1st ed. Portugal: Springer Berlin Heidelberg, 2014, 147 pp.

[22] M. Donachie, *Titanium: A technical guide, 2nd edition*. ASM International, 2000, 381 pp.

[23] Outokumpu. (2013). Handbook of Stainless Steel, [Online]. Available: http://www.outokumpu.com/sitecollectiondocuments/outokumpu-stainless-steel-handbook.pdf (visited on Jul. 26, 2016).

[24] SFS-EN 573-1, "Aluminium and aluminium alloys. Chemical composition and form of wrought products", Finnish standards association SFS, Standard, 2005.

[25] SFS-EN ISO 7599, "Anodizing of aluminium and its alloys. General specifications for anodic oxidation coatings on aluminium", Finnish standards association SFS, Standard, 2010.

[26] C. Vargel, "Chapter B.1 - Introducton to The Corrosion of Aluminium", in *Corrosion of Aluminium*, Amsterdam: Elsevier, 2004, pp. 81–109.

[27] B. D. Mert, B. Yazici, T. Tüken, G. Kardaş, and M. Erbil, "Anodizing and corrosion behaviour of aluminium", *Protection of Metals and Physical Chemistry of Surfaces*, vol. 47, no. 1, pp. 102–107, 2011.

[28] T. Salmi and S. Pajunen, *Lujuusoppi*, 1st ed. Tampere: Klingendahl paino Oy, 2010, 462 pp.

[29] E. Oñate, *Structural analysis with the finite element method*, 1st ed. Barcelona: Springer Netherlands, 2009, 472 pp.

[30] Neste Oil. (2016). Neste OH Grease product page, [Online]. Available: https://www.neste.fi/tuote/neste-oh-grease (visited on Oct. 10, 2016).

[31] HIAB. (2016). nDurance coating, [Online]. Available: http://www.atlaspolar.com/media/material-handling-equipment/hiab/brochures/HIAB-nDurance.pdf (visited on Oct. 10, 2016).

[32] P. Albers, *Motion control in offshore and dredging*, 1st ed. Springer Netherlands, 2010, 316 pp.

[33] Forum energy technologies. (2016). General Function Valve Pack data sheet, [Online]. Available: http://www.f-e-t.com/images/uploads/data-sheets/General_Function_Valve_Pack.pdf (visited on Sep. 28, 2016).

A. FINAL DESIGN OF THE 6 DOF UNDERWATER MANIPULATOR

B. PAYLOAD CALCULATION

Initial values

	Mass	COG from the boom tip
Link 4	$m_{L4} := 5.6kg$	$l_{L4} := 89mm$
Link 5	$m_{L5} := 13.4kg$	$l_{L5} := 571mm$
Link 6	$m_{L6} := 15.3kg$	$l_{L6} := 765mm$
Link 7	$m_{L7} := 2.5kg$	$l_{L7} := 1245mm$
Joint 5	$m_{J5} := 57.675kg$	$l_{J5} := 308mm$
Joint 6	$m_{J6} := 43.739kg$	$l_{J6} := 662mm$
Joint 7	$m_{J7} := 57.675kg$	$l_{J7} := 1048mm$
	$m_{max\_HIAB} := 540kg$	$l_{HIAB} := 4700mm$

$l_{wrist} := 1280$

$l_{load}(x) := (l_{wrist} + x)mm$

Maximum torque for HIAB 033

$M_{max\_HIAB} := m_{max\_HIAB} \cdot g \cdot l_{HIAB} = 2.489 \times 10^4 \cdot N \cdot m$

Torque output of the links and joints (origin at HIAB base)

$M_{L1} := m_{L4} \cdot g \cdot (l_{L4} + l_{HIAB}) = 262.999 \cdot N \cdot m$ $\quad M_{J5} := m_{J5} \cdot g \cdot (l_{J5} + l_{HIAB}) = 2.833 \times 10^3 \cdot N \cdot m$

$M_{L2} := m_{L5} \cdot g \cdot (l_{L5} + l_{HIAB}) = 692.657 \cdot N \cdot m$ $\quad M_{J6} := m_{J6} \cdot g \cdot (l_{J6} + l_{HIAB}) = 2.3 \times 10^3 \cdot N \cdot m$

$M_{L3} := m_{L6} \cdot g \cdot (l_{L6} + l_{HIAB}) = 819.978 \cdot N \cdot m$ $\quad M_{J7} := m_{J7} \cdot g \cdot (l_{J7} + l_{HIAB}) = 3.251 \times 10^3 \cdot N \cdot m$

$M_{L4} := m_{L7} \cdot g \cdot (l_{L7} + l_{HIAB}) = 145.751 \cdot N \cdot m$

Maximum payload

$M_{load} := M_{max\_HIAB} - M_{L1} - M_{L2} - M_{L3} - M_{L4} - M_{J5} - M_{J6} - M_{J7} = 1.458 \times 10^4 \cdot N \cdot m$

$$F_{load}(x) := \frac{M_{load}}{l_{load}(x) + l_{HIAB}}$$

$$m_{load}(x) := \frac{F_{load}(x)}{g} \qquad m_{load}(0) = 248.694\ kg$$

Maximum payload calculated using the second Eckart E3 actuator as limiting component:

$M_{max\_E3} := 2500N \cdot m$

$l_{load\_E3}(x) := (620 + x)mm$

Center of mass distance from the Eckart E3 actuator

$l_{L6\_2} := 104mm$ $\quad l_{L7\_2} := 584mm$ $\quad l_{J7\_2} := 387mm$

$M_{load\_E3} := M_{max\_E3} - g \cdot m_{L6} \cdot l_{L6\_2} - g \cdot m_{J7} \cdot l_{J7\_2} - m_{L7} \cdot g \cdot l_{L7\_2} = 2.251 \times 10^3 \cdot N \cdot m$

$$F_{load\_E3}(x) := \frac{M_{load\_E3}}{l_{load\_E3}(x)}$$

$$m_{load\_E3}(x) := \frac{F_{load\_E3}(x)}{g} \qquad m_{load\_E3}(0) = 370.254\ kg$$

$x := 0, 0.1 .. 600$

Payload capacity of the spherical wrist based on the payload capacities of HIAB loader crane and joint 6 Eckart E3 actuator

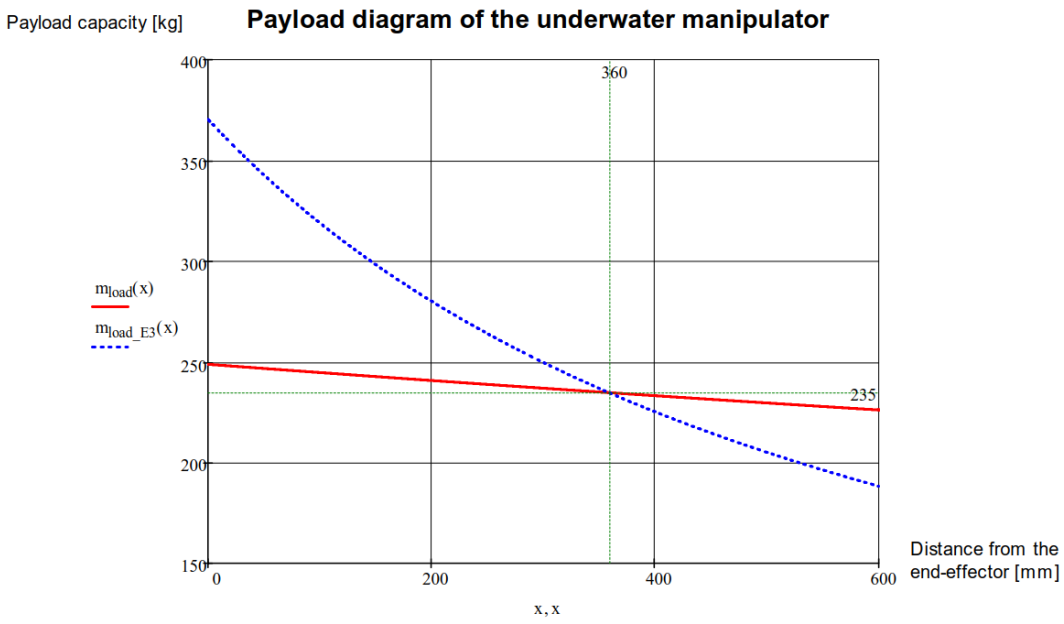

C. WORST CASE LOAD SCENARIO

Worst case load scenario

Initial values $d_3 := 0$ $\alpha := 32deg$ $\beta := 0deg$

Link length	Mass	Distance of COG
$L_2 := 1920mm$	$m_2 := 105kg$	$L_{cg2} := \frac{L_2}{2} = 0.96\,m$
$L_3(d_3) := (1770 + d_3)mm$	$m_3 := 180kg$	$L_{cg3}(d_3) := \frac{L_3(d_3)}{2}$ $L_{cg3}(d_3) = 0.885\,m$
$L_4 := 466.4mm$	$m_4 := 63kg$	$L_{cg4} := 290.6mm$
$L_5 := 195mm$	$m_5 := 56.2kg$	$L_{cg5} := 174mm$
$L_6 := 543mm$	$m_6 := 72.9kg$	$L_{cg6} := 334mm$
$L_7 := 74mm$	$m_7 := 2.4kg$	$L_{cg7} := 39.2mm$
	$m_{Ld} := 220kg$	
	$m_{max\_HIAB1} := 780kg$	

Gravitational forces of links

$G_4 := m_4 \cdot g$

$G_5 := m_5 \cdot g$

$G_6 := m_6 \cdot g$

$G_7 := m_7 \cdot g$

Hiab COG components (x and y)

$x_{cg2}(\alpha) := L_{cg2} \cdot \cos(\alpha)$	$x_{cg2}(\alpha) = 0.814\,m$
$x_2(\alpha) := L_2 \cdot \cos(\alpha)$	$x_2(\alpha) = 1.628\,m$
$x_{cg3}(\alpha, \beta, d_3) := x_2(\alpha) + L_{cg3}(d_3) \cdot \cos(\beta)$	$x_{cg3}(\alpha, \beta, d_3) = 2.513\,m$
$x_3(\alpha, \beta, d_3) := x_2(\alpha) + L_3(d_3) \cdot \cos(\beta)$	$x_3(\alpha, \beta, d_3) = 3.398\,m$
$x_{cg4}(\alpha, \beta, d_3) := x_3(\alpha, \beta, d_3) + L_{cg4} \cdot \cos(\beta)$	$x_{cg4}(\alpha, \beta, d_3) = 3.689\,m$
$x_4(\alpha, \beta, d_3) := x_3(\alpha, \beta, d_3) + L_4 \cdot \cos(\beta)$	$x_4(\alpha, \beta, d_3) = 3.865\,m$
$x_{cg5}(\alpha, \beta, d_3) := x_4(\alpha, \beta, d_3) + L_{cg5} \cdot \cos(\beta)$	$x_{cg5}(\alpha, \beta, d_3) = 4.039\,m$
$x_5(\alpha, \beta, d_3) := x_4(\alpha, \beta, d_3) + L_5 \cdot \cos(\beta)$	$x_5(\alpha, \beta, d_3) = 4.06\,m$
$x_{cg6}(\alpha, \beta, d_3) := x_5(\alpha, \beta, d_3) + L_{cg6} \cdot \cos(\beta)$	$x_{cg6}(\alpha, \beta, d_3) = 4.394\,m$
$x_6(\alpha, \beta, d_3) := x_5(\alpha, \beta, d_3) + L_6 \cdot \cos(\beta)$	$x_6(\alpha, \beta, d_3) = 4.603\,m$
$x_{cg7}(\alpha, \beta, d_3) := x_6(\alpha, \beta, d_3) + L_{cg7} \cdot \cos(\beta)$	$x_{cg7}(\alpha, \beta, d_3) = 4.642\,m$
$x_{Ld}(\alpha, \beta, d_3) := x_6(\alpha, \beta, d_3) + L_7 \cdot \cos(\beta)$	$x_{Ld}(\alpha, \beta, d_3) = 4.677\,m$
$y_{Ld}(\alpha, \beta, d_3) := L_2 \cdot \sin(\alpha) + \tan(\beta) \cdot (x_{Ld}(\alpha, \beta, d_3) - x_2(\alpha))$	$y_{Ld}(\alpha, \beta, d_3) = 1.017\,m$

Maximum torque to Joint 2

$M_{Joint2}(\alpha, \beta, d_3) := g \cdot (m_2 \cdot x_{cg2}(\alpha) + m_3 \cdot x_{cg3}(\alpha, \beta, d_3) + x_3(\alpha, \beta, d_3) \cdot m_{max\_HIAB1})$ $M_{Joint2}(\alpha, \beta, d_3) = 31.269 \cdot kN \cdot m$

Maximum force to lift cylinder

Lift cylinder dimensios

$\gamma := 13.3deg$ $L_{liftA\_J2} := 1120mm$ $L_{J2\_LiftB} := 320mm$ $L_{liftA\_J2\_y} := 1095mm$

Force to lift cylinder

$$F_{lift} := \frac{M_{Joint2}(\alpha, \beta, d_3)}{L_{J2\_LiftB}} = 97.714 \cdot kN$$

Cylinder position and stroke based on lift boom angle

$$c_{lift}(\alpha) := \sqrt{L_{liftA\_J2}^{2} + L_{J2\_LiftB}^{2} - 2 \cdot L_{liftA\_J2} \cdot L_{J2\_LiftB} \cdot \cos[\alpha + (90 - \gamma)]} \qquad c_{lift}(\alpha) = 1.366\,m$$

$$L_{lift\_y}(\alpha) := L_{J2\_LiftB} \cdot \sin(\alpha) + L_{liftA\_J2\_y} \qquad L_{lift\_y}(\alpha) = 1.265\,m$$

$$\beta_{Lift\_axial}(\alpha) := \operatorname{acos}\left(\frac{L_{liftA\_J2}^{2} - L_{J2\_LiftB}^{2} - c_{lift}(\alpha)^{2}}{-2 \cdot c_{lift}(\alpha) \cdot L_{J2\_LiftB}}\right) \qquad \beta_{Lift\_axial}(\alpha) = 35.2 \cdot deg$$

Torque from lift cylinder to joint 2

$F_{lift\_perp}(\alpha) := F_{lift} \cdot \sin(\beta_{Lift\_axial}(\alpha))$ $F_{lift\_perp}(\alpha) = 5.633 \times 10^{4} \cdot N$

$M_{lift}(\alpha) := F_{lift\_perp}(\alpha) \cdot L_{J2\_LiftB}$ $M_{lift}(\alpha) = 18.024 \cdot kN \cdot m$

Worst case load of the links

Moments caused by link weights (origin at joint 2)

$M_{Link2}(\alpha) := m_2 \cdot g \cdot x_{cg2}(\alpha)$ $M_{Link2}(\alpha) = 838.304 \cdot N \cdot m$

$M_{Link3}(\alpha, \beta, d_3) := m_3 \cdot g \cdot x_{cg3}(\alpha, \beta, d_3)$ $M_{Link3}(\alpha, \beta, d_3) = 4.436 \times 10^{3} \cdot N \cdot m$

$M_{Link4}(\alpha, \beta, d_3) := m_4 \cdot g \cdot x_{cg4}(\alpha, \beta, d_3)$ $M_{Link4}(\alpha, \beta, d_3) = 2.279 \times 10^{3} \cdot N \cdot m$

$M_{Link5}(\alpha, \beta, d_3) := m_5 \cdot g \cdot x_{cg5}(\alpha, \beta, d_3)$ $M_{Link5}(\alpha, \beta, d_3) = 2.226 \times 10^{3} \cdot N \cdot m$

$M_{Link6}(\alpha, \beta, d_3) := m_6 \cdot g \cdot x_{cg6}(\alpha, \beta, d_3)$ $M_{Link6}(\alpha, \beta, d_3) = 3.141 \times 10^{3} \cdot N \cdot m$

$M_{Link7}(\alpha, \beta, d_3) := m_7 \cdot g \cdot x_{cg7}(\alpha, \beta, d_3)$ $M_{Link7}(\alpha, \beta, d_3) = 109.25 \cdot N \cdot m$

$$M_{tot}(\alpha, \beta, d_3) := M_{Link2}(\alpha) + M_{Link3}(\alpha, \beta, d_3) + M_{Link4}(\alpha, \beta, d_3) + M_{Link5}(\alpha, \beta, d_3) + M_{Link6}(\alpha, \beta, d_3) + M_{Link7}(\alpha, \beta, d_3)$$

Sum of moments to the end-effector

$M_{RJ2}(\alpha, \beta, d_3) := M_{lift}(\alpha) - M_{tot}(\alpha, \beta, d_3)$ $M_{RJ2}(\alpha, \beta, d_3) = 4.994 \times 10^{3} \cdot N \cdot m$

Torque caused by maximum load

$M_{Load}(\alpha, \beta, d_3) := m_{Ld} \cdot g \cdot x_{Ld}(\alpha, \beta, d_3)$ $M_{Load}(\alpha, \beta, d_3) = 10.09 \cdot kN \cdot m$

Torque lever (Joint 1 -> end effector)

$$d_{Ld}(\alpha,\beta,d_3) := \sqrt{x_{Ld}(\alpha,\beta,d_3)^2 + (y_{Ld}(\alpha,\beta,d_3))^2} \qquad d_{Ld}(\alpha,\beta,d_3) = 4.786\,m$$

Angle of torque lever

$$alfa(\alpha,\beta,d_3) := atan\left(\frac{y_{Ld}(\alpha,\beta,d_3)}{x_{Ld}(\alpha,\beta,d_3)}\right) \qquad alfa(\alpha,\beta,d_3) = 12.274 \cdot deg$$

$$F_{R2}(\alpha,\beta,d_3) := \frac{M_{RJ2}(\alpha,\beta,d_3)}{d_{Ld}(\alpha,\beta,d_3)} \qquad F_{R2}(\alpha,\beta,d_3) = 1.044 \times 10^3 \cdot N$$

$$F_{R2x}(\alpha,\beta,d_3) := F_{R2}(\alpha,\beta,d_3) \cdot -\sin(alfa(\alpha,\beta,d_3)) \quad F_{R2x}(\alpha,\beta,d_3) = -221.843 \cdot N$$

$$F_{R2y}(\alpha,\beta,d_3) := F_{R2}(\alpha,\beta,d_3) \cdot \cos(alfa(\alpha,\beta,d_3)) \quad F_{R2y}(\alpha,\beta,d_3) = 1.02 \times 10^3 \cdot N$$

Force caused by Joint 1 (turn) to the end-effector

Maximum torque of the first joint (depending on working maximum working pressure)

$$M_{joint1} := 4665N \cdot m$$

$$F_{RJ1}(\alpha,\beta,d_3) := \frac{M_{Joint1}}{x_{Ld}(\alpha,\beta,d_3)} \qquad F_{RJ1}(\alpha,\beta,d_3) = 997.431 \cdot N$$ Reaction force reduced to end-effector

Forces to the end effector (direction according to manipulator axis)

$$F_1(\alpha,\beta,d_3) := \frac{F_{R2x}(\alpha,\beta,d_3)}{\cos(\beta)}$$

$$F_2(\alpha,\beta,d_3) := \frac{F_{R2y}(\alpha,\beta,d_3)}{\cos(\beta)}$$

$$F_3(\alpha,\beta,d_3) = F_{RJ1}(\alpha,\beta,d_3)$$

$$F_R(\alpha,\beta,d_3) := \sqrt{F_1(\alpha,\beta,d_3)^2 + F_2(\alpha,\beta,d_3)^2 + F_3(\alpha,\beta,d_3)^2} \qquad F_R(\alpha,\beta,d_3) = 1.444 \times 10^3 \cdot N$$

Maximizing force resultant

Given

$0 \le d_3 \le 1300$

$-20deg \le \alpha < 90deg$

$-45deg \le \beta \le 0deg$

$\beta \le \alpha$

$-2500mm \le y_{Ld}(\alpha, \beta, d_3)$

$Max_{values} := Maximize(F_R, \alpha, \beta, d_3)$ $\quad Max_{values} = \begin{pmatrix} -0.18 \\ -0.785 \\ 0 \end{pmatrix}$

$\alpha_{max} := Max_{values_0}$ $\quad \alpha_{max} = -10.335 \cdot deg$

$\beta_{max} := Max_{values_1}$ $\quad \beta_{max} = -45 \cdot deg$

$d_{3max} := Max_{values_2}$ $\quad d_{3max} = 0$

$F_R(\alpha_{max}, \beta_{max}, d_{3max}) = 5.279 \times 10^3 \cdot N$

$F_1(\alpha_{max}, \beta_{max}, d_{3max}) = 2.708 \times 10^3 \cdot N$

$F_2(\alpha_{max}, \beta_{max}, d_{3max}) = 4.382 \times 10^3 \cdot N$

$F_3(\alpha_{max}, \beta_{max}, d_{3max}) = 1.153 \times 10^3 \cdot N$

$F_1 := 2710N$

$F_2 := 4400N$

$F_3 := 1200N$

Values are used in Link 7 FEM calculation

Reaction forces, worst case load

Link 7 These loads are used in Link 6 FEM calculation

$R_1 := F_1$	$R_1 = 2.71 \times 10^3 \cdot N$	$M_{t1} := 0N \cdot m$	$M_{t1} = 0$
$R_2 := F_2 + m_7 \cdot g$	$R_2 = 4.424 \times 10^3 \cdot N$	$M_{t2} := F_3 \cdot L_7$	$M_{t2} = 88.8 \cdot N \cdot m$
$R_3 := F_3$	$R_3 = 1.2 \times 10^3 \cdot N$	$M_{t3} := F_2 \cdot L_7 + G_7 \cdot L_{cg7}$	$M_{t3} = 326.523 \cdot N \cdot m$

Link 6 These loads are used in Link 5 FEM calculation

$R_4 := R_1$	$R_4 = 2.71 \times 10^3 \cdot N$	$M_{t4} := 0N \cdot m$	$M_{t4} = 0$
$R_5 := R_2 + m_6 \cdot g$	$R_5 = 5.138 \times 10^3 \cdot N$	$M_{t5} := R_3 \cdot L_6 + M_{t2}$	$M_{t5} = 740.4 \cdot N \cdot m$
$R_6 := R_3$	$R_6 = 1.2 \times 10^3 \cdot N$	$M_{t6} := R_2 \cdot L_6 + G_6 \cdot L_{cg6} + M_{t3}$	$M_{t6} = 2.967 \times 10^3 \cdot N \cdot m$

Link 5 These loads are used in Link 4 FEM calculation

$R_7 := R_4$	$R_7 = 2.71 \times 10^3 \cdot N$	$M_{t7} := 0N \cdot m$	$M_{t7} = 0$
$R_8 := R_5 + m_5 \cdot g$	$R_8 = 5.69 \times 10^3 \cdot N$	$M_{t8} := R_6 \cdot L_5 + M_{t5}$	$M_{t8} = 974.4 \cdot N \cdot m$
$R_9 := F_3$	$R_9 = 1.2 \times 10^3 \cdot N$	$M_{t9} := R_5 \cdot L_5 + G_5 \cdot L_{cg5} + M_{t6}$	$M_{t9} = 4.065 \times 10^3 \cdot N \cdot m$

Link 4

$R_{10} := F_1$	$R_{10} = 2.71 \times 10^3 \cdot N$	$M_{t10} := 0N \cdot m$	$M_{t10} = 0$
$R_{11} := R_8 + m_4 \cdot g$	$R_{11} = 6.307 \times 10^3 \cdot N$	$M_{t11} := R_9 \cdot L_4 + M_{t8}$	$M_{t11} = 1.534 \times 10^3 \cdot N \cdot m$
$R_{12} := F_3$	$R_{12} = 1.2 \times 10^3 \cdot N$	$M_{t12} := R_8 \cdot L_4 + G_4 \cdot L_{cg4} + M_{t9}$	$M_{t12} = 6.898 \times 10^3 \cdot N \cdot m$

D. HYDRAULIC DIAGRAM OF THE 6 DOF UNDERWATER MANIPULATOR

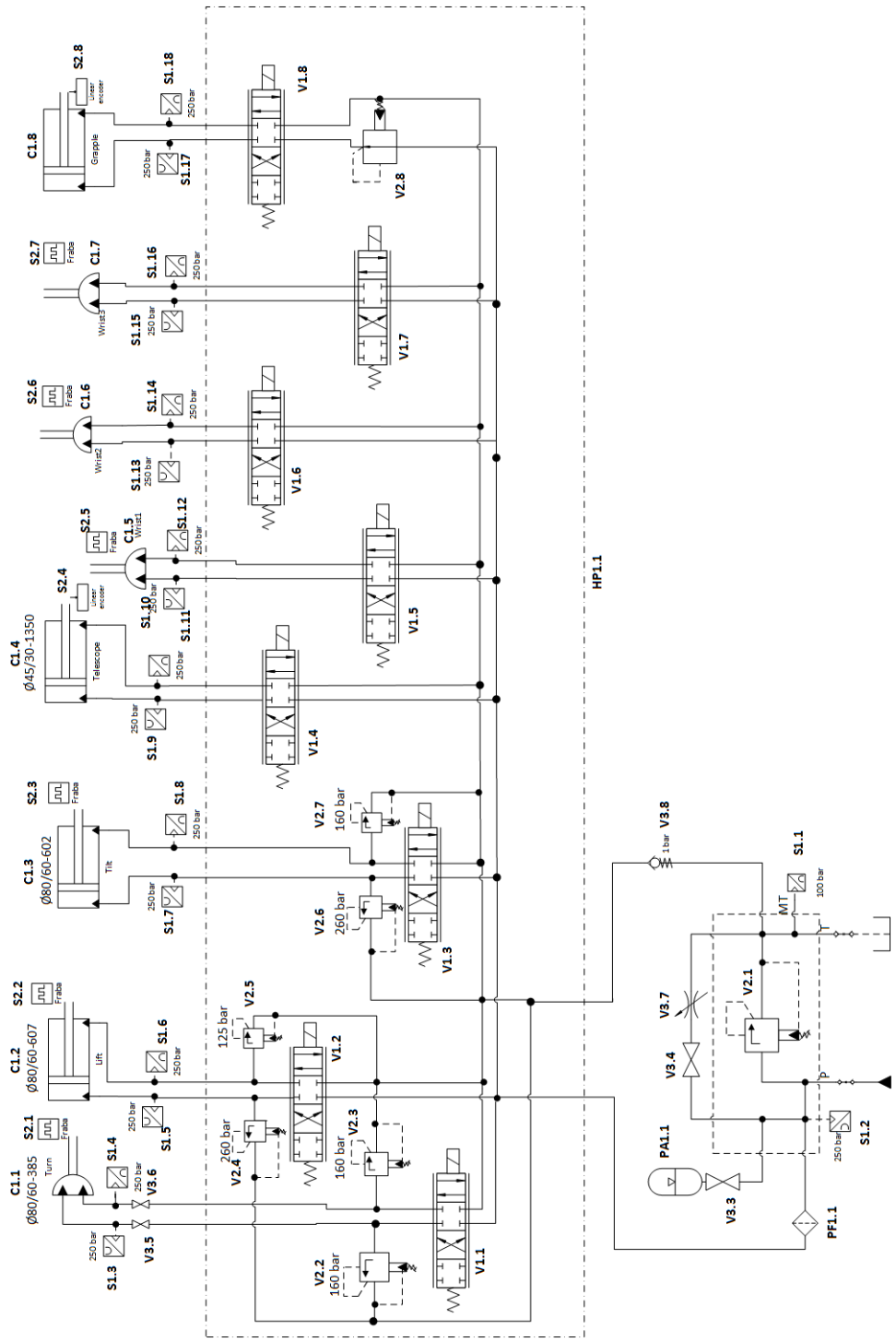

Part number	Component	Data	Other information
V1.1-V1.8	Control valve	Bosch Rexroth BR 4WPREH 6 C4 B40L	
S1.1,S1.3-S1.8,S1.11-S1.18	Pressure transmitter 250 bar	Druck PTX 1400 4-20 mA	
S1.8-S1.10	Pressure transmitter 250 bar	Druck UNIK 5000 4-20 mA	
S1.2	Pressure transmitter 400 bar	Druck PTX 1400 4-20 mA	
PA1.1	Pressure accumulator	20 L/330 bar	
V3.7	Ball valve	DN20/PN250	
V3.4-V3.6	Ball valve	DN6/250 bar	
V3.3	Ball valve	DN20/PN250 with 1 bar spring	
V2.1-V2.7	Sandwitch plate	SUN RPCCLAN-ABX pressure relief	
V2.8	Sandwitch plate	SUN PBDBLAN-EBP pressure reducing	
S2.4	WS11 Position Sensor with Incremental Encoder	Stegmann DG 60 L Incremental Encoder	4096 puls/rev
PF1.1	Pressure filter	ACRO 375 93 000	
HP1.1	Hydraulic plate	8 x ISO 4401-03-02-0-05	
S2.1-S2.3,S2.5-S2.7	Incremental encoder	Fraba UCD-INS01-6384-D10D-ARW	16384 puls/rev
C1.2	Lift cylinder	Ø80/60-607	
C1.3	Tilt cylinder	Ø80/60-602	
C1.4	Extension cylinder	Ø45/30-1350	
C1.1	Swing cylinder	Ø80/60-385	
S2.8			
C1.5	Eckart E3 hydraulic rotary actuator	360deg/2500Nm	
C1.6	Eckart E3 hydraulic rotary actuator	180deg/2500Nm	
C1.7	Eckart E3 hydraulic rotary actuator	360deg/2500Nm	